

Tactile Sensors for Friction Estimation and Incipient Slip Detection—Toward Dexterous Robotic Manipulation: A Review

Wei Chen, Heba Khamis^{ID}, Member, IEEE, Ingvars Birznieks, Nathan F. Lepora^{ID}, and Stephen J. Redmond^{ID}, Senior Member, IEEE

Abstract—Humans can handle and manipulate objects with ease; however, human dexterity has yet to be matched by artificial systems. Receptors in our fingers and hands provide essential tactile information to the motor control system during dexterous manipulation such that the grip force is scaled to the tangential forces according to the coefficient of friction. Likewise, tactile sensing will become essential for robotic and prosthetic gripping performance as applications move toward unstructured environments. However, most existing research ignores the need to sense the frictional properties of the sensor–object interface, which (along with contact forces and torques) is essential for finding the minimum grip force required to securely grasp an object. Here, we review this problem by surveying the field of tactile sensing from the perspective that sensors should: 1) detect gross slip (to adjust the grip force); 2) detect incipient slip (dependent on the frictional properties of the sensor–object interface and the geometries and mechanics of the sensor and the object) as an indication of grip security; or 3) measure friction on contact with an object and/or following a gross or incipient slip event while manipulating an object. Recommendations are made to help focus future sensor design efforts toward a generalizable and practical solution to sense, and hence control grip security. Specifically, we propose that the sensor mechanics should encourage incipient slip, by allowing parts of the sensor to slip while other parts remain stuck, and that instrumentation should measure displacement and deformation to complement conventional force, pressure, and vibration tactile sensing.

Index Terms—Friction, grip, manipulation, sensors, slip, tactile.

I. INTRODUCTION

ROBOTS traditionally operate in structured environments performing repetitive pre-programmed movements, such

Manuscript received July 4, 2018; revised August 28, 2018; accepted August 29, 2018. Date of publication September 3, 2018; date of current version October 23, 2018. This work was supported by the Australian Research Council Future Fellowships under Grant FT130100858. The associate editor coordinating the review of this paper and approving it for publication was Dr. Rosario Morello. (*Wei Chen and Heba Khamis contributed equally to this work.*) (*Corresponding author: Heba Khamis.*)

W. Chen, H. Khamis, and S. J. Redmond are with the Graduate School of Biomedical Engineering, University of New South Wales, Sydney, NSW 2052, Australia (e-mail: wei.chen6@unsw.edu.au; h.khamis@unsw.edu.au; s.redmond@unsw.edu.au).

I. Birznieks is with the School of Medical Sciences, University of New South Wales, Sydney, NSW 2052, Australia (e-mail: i.birznieks@unsw.edu.au).

N. F. Lepora is with the Department of Engineering Mathematics, University of Bristol, Bristol BS8 1QU, U.K., and also with the Bristol Robotics Laboratory, University of Bristol, Bristol, U.K. (e-mail: n.lepora@bristol.ac.uk).

Digital Object Identifier 10.1109/JSEN.2018.2868340

as production line assembly. More recently, however, they are finding use in unstructured environments where robotic grippers are required to perform increasingly human-like manipulation tasks (e.g., picking up novel, fragile objects). Studies of humans [1] and monkeys [2] have shown that mechanoreceptors in the fingers play a critical role in providing information about an object's shape, weight, and mass distribution [3]–[5], and without feedback from these receptors even simple object manipulation tasks become difficult [6]–[8]. Therefore, it is generally recognized that providing robotic grippers with feedback via tactile sensors is an essential step for improving their dexterity, towards human-like performance.

While research on tactile sensing dates back to the 1970s, artificial tactile sensors aimed at improving robotic gripping still fall far short of the capabilities of their biological counterparts [9]. The vast majority of reported tactile sensors for robotic applications have focused on transducing one or more basic physical properties of the object-gripper interface, such as forces, pressure, displacement, vibration, and temperature [10]–[12], with many being based on arrays of pressure-sensitive tactile elements (taxels). However, the crucial property of friction, and the parameters it influences, has been largely ignored.

Friction is the resistance to relative sliding or rolling movement between two objects in contact. The friction encountered in most robotic gripping operations are static and kinetic dry solid sliding friction. The coefficient of static (kinetic) friction, μ_s (μ_k), is equal to the ratio of the minimum tangential force needed to initiate sliding (maintain sliding at a constant velocity) to the normal force. It is μ_s at the gripper-object contact interface that determines the minimum grip force required to hold an object of a given weight. Therefore, friction plays a vital role in dexterous manipulation tasks.

Classical studies of friction have considered that μ_s is a constant for a pair of materials in contact. However, the modern view is that μ_s is both material- and system-dependent. For a pair of materials in contact, μ_s and μ_k can vary with normal load, sliding velocity, apparent contact area, environmental factors such as temperature and humidity [13]–[15], age of contact, and rate of change of tangential force [16]. Also, μ_s may not encode the force threshold required to initiate movement across all velocity scales [17]–[19]. Therefore, in applications where friction plays a key role, there is a strong motivation for the use of real-time friction-based sensing.

Friction (or friction-related) information at the object-gripper interface can be sensed in various ways to improve object manipulation. One approach is to estimate μ_s by allowing gross slip to occur and then measure the tangential and normal forces at the onset of this gross slip; i.e., when relative sliding motion between the sensor and the object starts. A second approach is to measure μ_s when the gripper first contacts the object, but before it attempts to lift the object. A final approach involves detecting incipient slip (when part of the sensor-object interface (SOI) slips while other parts remain stuck); the measurement of friction here is not necessarily explicit, but frictional information is signaled when regions of the contact area slip. For general manipulation tasks, all of these approaches may be needed.

This paper aims to review tactile sensors that directly or indirectly utilize friction information to improve grip security. Friction sensing is a subset of tactile sensing, and while valuable review papers on tactile sensors are periodically published in the literature [9], [10], [20]–[26], this is the first to provide a comprehensive review of tactile sensors in the context of friction and grip security estimation. This review starts with an explanation of human tactile sensing of friction-related information (human-like dexterous manipulation is considered the ultimate capability which artificial tactile sensing aims to facilitate); the literature on artificial friction-based tactile sensing methods is then covered; finally, our conclusions compare existing competing approaches and make recommendations for future research.

II. HUMAN SENSE OF TOUCH

Much effort has been invested in developing tactile sensors that enable artificial grippers to replicate the function of the human hand/fingers. Given that artificial tactile sensors often aspire to emulate human touch, a brief review of the physiology and biomechanics of human tactile sensing are introduced here as preface to the review of sensors to follow.

A. Physiology of Human Tactile Sensing

1) Tactile Mechanoreceptors and Afferents: The human sense of touch is mediated by four types of mechanoreceptors that are embedded in the skin. There are $\sim 17,000$ mechanoreceptors in the grasping surfaces (glabrous, i.e., non-hairy, skin) of the human hand, and the highest density ($\sim 240 \text{ cm}^{-2}$) of these mechanoreceptors are found in the fingertip (distal half of the finger pad) [1]. The mechanoreceptors are innervated by four types of tactile afferents: two types respond to static stimuli with a sustained discharge (slowly adapting; SA), and two types only respond transiently to changing stimuli (fast adapting; FA) [1]. Afferents are further classified as Type I (small receptive fields with distinct borders), or Type II, (receptive fields which lack distinct borders) [1]. Thus, the glabrous skin of the human hand contains SA Type I (SAI), SA Type II (SAII), FA Type I (FAI) and FA Type II (FAII) afferents. These respond predominantly to pressure, stretch, and vibration and recent evidence shows that most afferent classes are excited by most tactile stimuli [27]. Tactile information is signaled to the central nervous system and utilized

during object manipulation; although how this information is decoded is still under investigation [5], [27]–[29].

2) Biomechanics of the Skin: While the mechanoreceptors (and their associated afferents) sense, encode, and transfer tactile signals, the skin is vital to the sensing process as it converts the dynamics of the skin-object interaction into stresses and deformations which encode information about both the properties of the object and the interface between the skin and the object (i.e., friction and/or grip security). Human skin is multilayered, viscoelastic, nonhomogeneous, and has a nonlinear stress-strain response [30]–[32]. The glabrous skin of the human finger pad is characterized by the fingerprint ridges and a high density of sweat glands [14], [33]. There is evidence that the fingerprint ridges improve tactile sensation by amplifying mechanical stimuli for mechanoreceptor excitation [34]. There is further support for this from artificial tactile sensors [35], [36]. However, fingerprint ridges may serve several different functions simultaneously, including mitigating the risk of delamination of the skin (i.e., preventing blisters) [34]. Sweat excretion changes the fingertip wetness to minimize the required grip forces during object manipulation [14], [15], [37], indicating that skin-object friction is rarely constant in the strictest sense.

3) Grip Force Control: During object manipulation, humans automatically apply forces normal to the grasped surface in proportion to the tangential load force, but scaled by μ_s at the skin-object interface [7]. Importantly, it is friction, rather than texture, that is the primary determinant in the control of grip force [38]. When friction is considerably reduced, after subjects wash their hands with soap, the grip force used when lifting an object increases, reflecting the demands of reduced friction; and over repeated trials, the grip force decreases as the friction increases due to sweat production [39]. When an object (varying weights, surface texture and friction) is held between the thumb and index finger, the grip force is always larger than the slip force (minimum grip force) so that the object does not slip, and the grip force is not excessive [8]. Also, the ability of subjects to perform manipulation tasks is diminished when the skin of the fingertip is anaesthetized, demonstrating the reliance on tactile sensory information [6]–[8].

Both the complex mechanical structure and properties of the glabrous skin, along with the large number of different types of embedded mechanoreceptors, contribute to human tactile sensation. This tactile sensory information is crucial for maintaining sufficient but not excessive forces and helps to securely grasp an object during dexterous manipulation.

B. Friction Sensing on Initial Contact

One mechanism by which it is proposed that humans can sense friction is on initial contact with an object via microslips (spatially-localized stick-slip events). For more slippery surfaces, shear (tangential) stress at the skin-object interface is released when microslips occur (skin slips on the object surface) as the grip (normal) force increases [40]. Such shear stress develops from the center to the periphery along radial axes because the fingertip is approximately hemispherical.

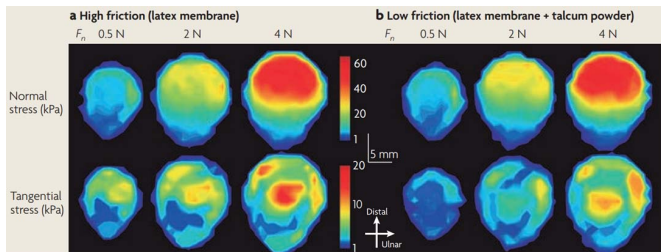


Fig. 1. Distributions of normal and tangential stresses when the fingerpad contacts a stationary surface at three normal force levels (F_n) for (a) a high and (b) a low friction surface. Similar normal stresses are observed in both friction conditions. Lower overall tangential stress is observed for the low friction surface due to lower frictional forces; that is, there is more localized slipping (microslips) in the contact area for the more slippery surface. Reproduced from [40] with permission from Macmillan (Copyright 2009).

For a low friction surface, more microslips are presumed to occur due to the lower frictional forces which allow the shear stress to be released as the grip force increases; for a high friction surface, the larger frictional forces prevent the occurrence of microslips and therefore larger shear stresses are observed (Fig. 1). While the observed shear stresses in the fingerpad support the view that humans may be able to sense friction on initial contact with the object, microslips have not yet been experimentally observed – experiments to observe such events would be extremely difficult to carry out – and only a few studies have investigated afferent responses to different frictional conditions on initial contact, discussed below.

Johansson and Westling [41] showed that early adjustment (~ 100 ms after contact with an object) to a new frictional condition may depend on the FAI unit responses during the lifting phase of object manipulation. However, the experiment did not conclusively determine whether this response was due to friction or texture. Also, the tangential load increased in parallel with the normal force as soon as initial contact was made, therefore the subjects may be using cues from incipient slips to adjust the grip force.

Khamis *et al.* [42] demonstrated that tactile afferent responses are modulated by friction. Friction could be classified with over 80% accuracy using spike count features from each afferent in the population (5 SAI, 5 FAI, 2 SAII and 2 FAII). A normal force was applied to the subject's fingerpad using different 3D-printed textured surfaces treated with friction increasing and decreasing agents, thus overcoming the previous limitations of being unable to disentangle the effects of texture and friction. The results support the idea that at initial contact with an object (before a tangential load is applied), the human sensory system is influenced by friction-dependent changes in skin deformation patterns.

While these studies indicate that some friction information can be sensed at the initial contact with an object, this has not yet been shown conclusively. Furthermore, the friction of the fingerpad skin is affected by normal force and hydration [14], [15], [37], [43], contact area, surface roughness, motion direction and sliding speed [44]. Additionally, for some materials the friction increases dramatically after the grasp is initiated, due to the reconfiguration of keratin molecules at the interface, meaning that an estimate of low friction made

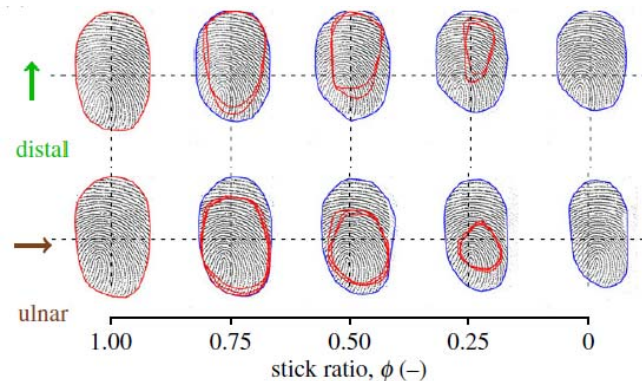


Fig. 2. Evolution of the stuck area for a human fingerpad. Example images for stick ratios of 1 (entire contact area is stuck), 0.75, 0.5 (half the contact area is slipping), 0.25 and 0 (entire contact area is slipping) for distal and ulnar shearing of a transparent glass plate for subject S3. Three trials (same normal force and speed) are superimposed. Background picture is the contact area from one trial. Contact (stuck) area is blue (red) contours. Reproduced from [46] with permission from The Royal Society (Copyright 2014).

at initial contact may lead to a substantial overestimation of the grip force required a few seconds later [45]. Therefore, while sensing friction at initial contact is beneficial for securely lifting an object, it may not be appropriate for ongoing maintenance of a secure grip. The evidence does not support the notion that the friction sensed on contact is the only friction-related information that humans use throughout the manipulation task.

C. Grip Security During Manipulation

The fingerpad allows for independent movement of skin regions – skin is able to stretch and compress tangential to its surface in localized regions [37], [46], [47]. The convex shape of the fingerpad also helps ensure that, when in contact with a surface with positive curvatures (e.g., a sphere), the skin at the periphery of the contact area is subject to a lower pressure. The skin at the periphery of the contact area is therefore more likely to experience slip when a tangential force is loaded, than the skin at the center of the contact area [37], [46]. The region of incipient slip around the periphery of the contact area grows as the tangential force is increased (Fig. 2). It has been proposed that, in humans, the ability to sense this incipient slip is important for maintaining grasp stability during manipulation tasks [41].

Khamis *et al.* [28] showed that the ratio of tangential-to-normal force can be estimated as a percentage of the critical load capacity (the maximum tangential-to-normal force ratio achieved before gross slip will occur) using the responses of only a small number of afferents. While this is evidence that we can sense grip security, the question of which biomechanical mechanism the tactile afferents are transducing remains to be answered. One possibility is that they are responding to incipient slip.

III. TACTILE SENSING TO IMPROVE ROBOTIC MANIPULATION

A. Review of Gross Slip, Incipient Slip, and Friction Sensors

Tactile sensing refers to the transduction of any type of information/signal through physical contact between the

sensor and an object. Many tactile sensing techniques have been proposed to improve robotic manipulation, most of which focus on contact force measurement or on slip detection; these have been reviewed in detail in the literature [10], [20], [21], [25], [26]. However, most of the existing research has not considered the need to sense the frictional properties of the SOI to maintain a firm grip. Adjusting the grip force to maintain a stable grasp while not crushing the object, is something humans do with ease; for robotic manipulation, one approach to achieve this level of dexterity would be to determine the coefficient of static friction (μ_s) while handling the object.

This section will review three main approaches to improve grip security during object manipulation by robotic grippers:

- (i) gross slip detection (when all parts of the contact interface slide against each other);
- (ii) incipient slip detection (when part of the contact interface slides while other parts remain stuck);
- (iii) friction estimation (performed either using gross or incipient slip detection during active exploration or during manipulation, or on initial contact with object).

All three of these categories involve slip detection. The major differences are the extent of slip required, and whether μ_s is estimated in order to inform a subsequent grip force adjustment, which will impact on the utility of the technique when employed in real-time manipulation tasks.

The sensors reviewed in this work are presented in Table 1. The table summarizes the main physical and transduction properties of the sensor, how it was validated, its performance, and the main advantages and disadvantages of the sensor. A brief description of the key design features of each sensor and the general advantages and disadvantages of different approaches are presented in the following subsections. In each subsection, the sensors are described in chronological order as well as by following the sensor design developments of a particular research group or developments in the application of a particular sensor (e.g., a commercially available sensor).

B. Gross Slip Detection

For two surfaces in contact (sensor surface and object surface), gross slip refers to the case when all parts of both contact surfaces slip completely against each other. If the object is already lifted, relying on gross slip detection to ensure grip security risks dropping the object if the slip cannot be arrested by sufficiently increasing the grip force; therefore, it should be considered a last resort after other methods of controlling grip security. Moreover, a previous review on artificial slip sensing has covered many of the various gross slip sensors [48]. For these reasons, this review will focus more on incipient slip and friction estimation. That being said, a number of gross slip sensors have been published since the review in [48], and there are some published sensors that are not covered by [48]. For completeness, both new and omitted papers on gross slip detection are briefly reviewed here.

Choi *et al.* [49] describe a fingertip tactile sensor composed of a force sensor (two overlaid polyester films with pressure-variable resistor ink forming a grid type electrode pattern) and

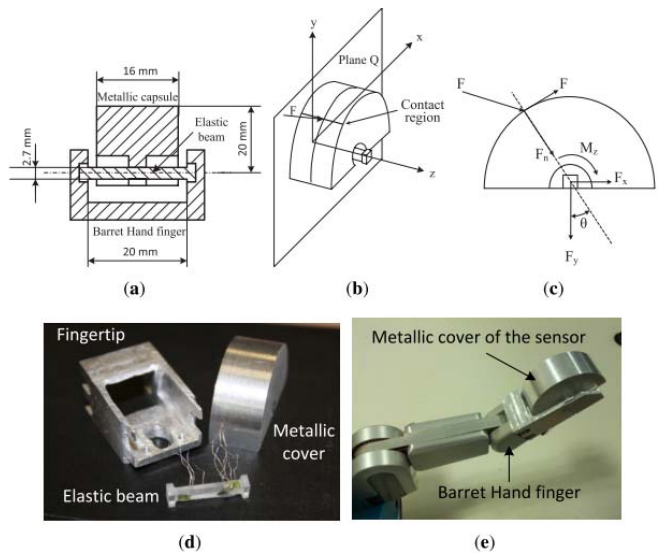


Fig. 3. Sensor for gross slip detection developed by Fernandez *et al.*: (a) Cross-section of the sensor; (b) applied force F ; (c) decomposition of applied force F ; (d) sensor parts; (e) sensor mounted on a BarrettHand finger. Reproduced from [53] with permission from MDPI (Copyright 2014).

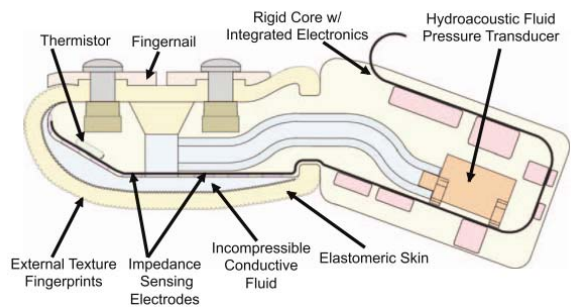


Fig. 4. Cross-sectional schematic of the BioTac sensor. Adapted from [57] with permission from IEEE (Copyright 2014).

a slip sensor (a single polyvinylidene difluoride (PVDF) film). Sharp changes in the PVDF film signal were thought to imply that stick-slip (gross slip) has occurred.

Two more published works used the Myrmex sensor – a matrix of 16×16 sensor cells, covered with a carbonized foam with a pressure dependent resistance [50]. Schöpfer *et al.* [51] used a neural network (NN) to estimate slip velocity from the frequency spectrum of the Myrmex sensor output. Meier *et al.* [52] applied a convolution NN to the short-time Fourier transform of signals from two Myrmex sensors (one on either side of a gripper) to classify the grip condition as stable, translational slip or rotational slip.

Fernandez *et al.* [53] developed a sensor with strain gauges that measure moments transmitted from a metallic semi-cylindrical cover to an elastic beam (Fig. 3). Slip induced structural micro-vibrations were detected when the product of the spectral peak value and peak frequency of the Fourier transform of the strain gauge signals exceeded a threshold.

A number of published works used the BioTac sensor (SynTouch, CA, USA; Fig. 4) – a multimodal tactile sensor, with a compliant elastomer fingertip filled with conductive

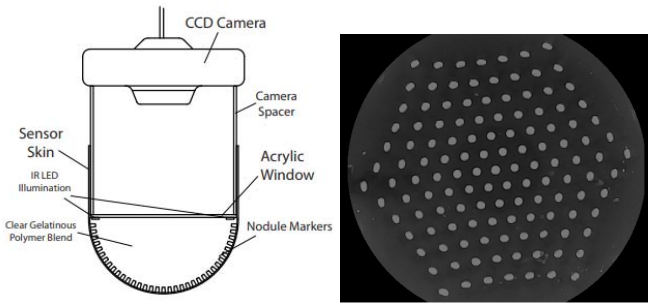


Fig. 5. (a) Cross-sectional schematic of the TacTip sensor. Adapted from [62] with permission from IEEE (Copyright 2009). (b) Raw camera image. Adapted from [61] with permission from IEEE (Copyright 2018).

fluid and a stiff fingernail on the back – for slip detection. The BioTac contains nineteen electrodes to measure inter-electrode fluid impedance as the fingertip skin is deformed, a hydrophone to transduce vibrations and a pressure sensor to measure the fluid pressure. Su *et al.* [54] proposed two methods for detecting gross slip using the BioTac: (i) a force-derivative method in which a slip is detected when the tangential force derivative (estimated from the fluid impedance) drops below a threshold; and (ii) a vibration-based method in which a slip is detected if more than half of the fluid pressure sensor values in a time window exceed a threshold which is twice as large as the baseline environmental vibration. Features from all the signals of the BioTac have also been used to predict gross slip [55] with prediction horizons of 0.005, 0.01, 0.015 and 0.02 s, using a random forest classifier, support vector machine, and spectral slip classifier.

Heyneman and Cutkosky [56] reported the performance of three tactile sensors with respect to classifying slip as occurring between a grasped object and the sensor, or between a grasped object and the world. Features relating to signal power and mean square coherence across all sensing element pairs were extracted from the BioTac [57], a sensor with an array of capacitive sensors and accelerometers [58], [59], and a PVDF-based sensor with a curved, textured rubber, outer skin. Similar slip-state classification was performed by [60] on features extracted from three unidentified sensors using a Long-Short-Term Memory NN. Classification accuracy was found to vary with sampling rate, window size, material, and slipping speed, with accuracies ranging from 57.6% to 93.7%.

The most recent gross slip detector in the literature is the TacTip [61] – a biomimetic optical tactile sensor that operates by tracking internal pins embedded in a compliant skin (Fig. 5). These pins provide a strong signal of gross slip as the direction of their velocities align at the moment of slip onset. A support vector machine classifier gave accurate discrimination (99.88%) between slipping and non-slipping, with robustness to object shape and rate of slip initiation. This was sufficient to arrest slipping objects before being dropped for movement constrained to the vertical direction only.

The sensors detecting gross slip that were reviewed in [48], and the further approaches reviewed here [49], [51]–[56], [61], detect gross slip by measuring displacement, vibrations, forces or thermal flows using piezoresistive, piezoelectric,

capacitive, optical and thermal transducers. An important aspect of grip security is how the grip force is to be adjusted following gross slip detection to recover the grasp on the object. A common proposal is to simply increase the grip force in a predetermined way until slip is no longer detected [63]–[69]. However, if gross slip detection is the only tactile sensing that is performed, it is not known how much the grip force needs to be adjusted to restore grip; determining the appropriate grip force adjustment is inextricably linked to measuring friction and forces at the gripping interface, either directly or indirectly. Furthermore, even if the magnitude of the grip force adjustment required is accurately determined, it remains to be seen whether gross slip can be detected early enough to allow enough time for grip force adjustment; in fact, this may not be possible in cases where the object need only slip a very small distance before it is dropped.

C. Incipient Slip Detection

Incipient slip refers to when part of the contact interface slides while other parts of the contact area remain stuck, and this occurs prior to gross slip. Therefore, detection of incipient slip is gaining recognition in the literature as a feasible mechanism for maintaining a secure grasp. These slips may be detected via associated localized vibrations at the periphery of the contact region, or as relative displacement of localized parts of the sensor surface. The key concept underpinning this approach is that part of the sensor can deform/slipp independently of the rest of the sensor due to it having appropriate mechanical compliance. The localized incipient slip is driven by differences in the forces experienced at different parts of the SOI, achieved by the sensor having appropriate shape with positive surface curvature. Detecting this incipient slip would indicate that the grip force needs to be increased to maintain a stable grip on the object, before gross slip takes place. The sensors that have been reported in the literature which detect incipient slip are described below.

Building on the work of Dornfield and Handy [70], who showed that slips produce ultrasonic emissions, Ando and Shinoda [71] proposed an ultrasonic emission tactile sensor made of a flexible, hemispheric body with an embedded PVDF sound sensing matrix. They showed that the ultrasonic emissions sources could be localized and propose that this mechanism may make the detection of incipient slip possible.

Marconi and Melchiorri [72] and Holweg *et al.* [73] developed a sensor made of a 16×16 array of conductive rubber with force-dependent resistance. As a tangential force is applied, before slip, the rubber is stretched and a small movement of the object causes a shift in the position of the center of the force distribution which they detect from the fast Fourier transform of 32 successive positions.

Maeno *et al.* [74] showed that the shear-strain distribution inside a curved elastic finger indicates the stick-slip pattern at the finger surface during gripping. Incipient slip always occurs near the edge of the contact area when the grasp is established due to the positive curvature of the elastic finger. A real elastic finger was made with embedded strain gauges (Fig. 6) [75] and the strain distribution pattern was similar to results from

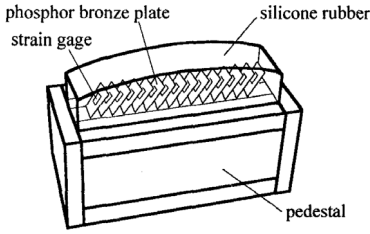


Fig. 6. Elastic curved finger developed by Maeno *et al.* Fifteen phosphor bronze plates of 0.1 mm thickness are embedded in an elastic body of silicone rubber at an angle of 45 degrees from the x-axis. Strain gages are bonded to the phosphor bronze plates. The strain distribution measured by the strain gauges can indicate a condition of incipient slip. Reproduced from [75] with permission from IEEE (Copyright 1998).

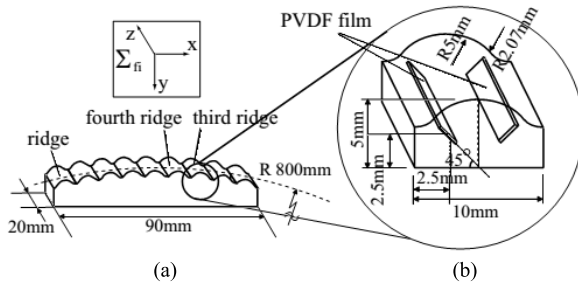


Fig. 7. Artificial finger skin, developed by Fujimoto *et al.* The dimensions of the whole sensor, each ridge as well as the location and orientation of the embedded strain gauges are described. The sensor has nine ridges on the surface and a pair of strain gauges is embedded underneath each ridge. Reproduced from [79] with permission from IEEE (Copyright 2003).

finite element analysis, indicating that it may be used to detect incipient slip. A method for using the elastic finger to adjust the grip force was also proposed [76]. The area of the stuck region is monitored by the change in shear strain inside the elastic finger and the slope of the normal to tangential curve is increased (decreased) when the stuck area is large (small). Yamada *et al.* [77] built on previous work [75], [78] to design an artificial elastic finger with a surface geometry imitating the ridges of the human finger. Incipient slip of the ridges at the edge of the contact area was detected by a change in the first and second time derivatives of the strain difference from two strain gauges embedded within each ridge. Fujimoto *et al.* [79] later replaced the strain gauges with PVDF films (Fig. 7), and a NN was trained to detect incipient slip.

Canepa *et al.* [80] described a tactile sensor consisting of a linear array of eight pairs of piezoelectric polymer transducers underneath a layer of silicone rubber. One transducer in each pair is sensitive to normal stress and the other to shear stress. The rate of change of normal and shear stress are used to train a NN to output the degree of incipient slip as the ratio of tangential force to the maximum allowable tangential force (measured offline) at which gross slip would occur; a similar ratio was described in [29] (see section II-C).

Ikeda *et al.* [81] and Ueda *et al.* [82] proposed a method of grip-force control based on feedback of a visual “slip margin”, determined from the deformation of an elastic surface (the object) against a flat transparent sensor. The slip margin (a custom index: 1 when the contact area is completely stuck, and 0 when the contact interface completely slips) is estimated

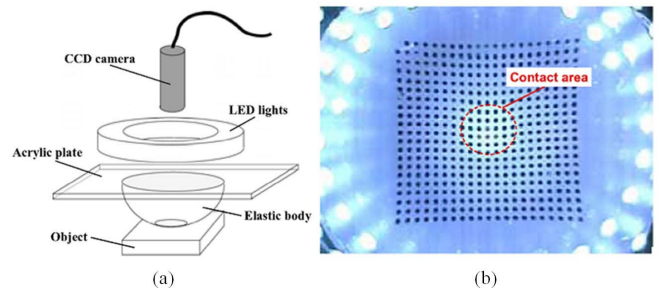


Fig. 8. Vision-based tactile sensor, developed by Watanabe and Obinata. (a) Structure of sensor, and (b) image captured by the camera during contact. The contact region is recognized by detecting the area having a brightness or light intensity greater than a predefined threshold. A stick ratio that indicates the degree of slippage is used to calculate the required grip force. Reproduced from [83] with permission from IEEE (Copyright 2007).

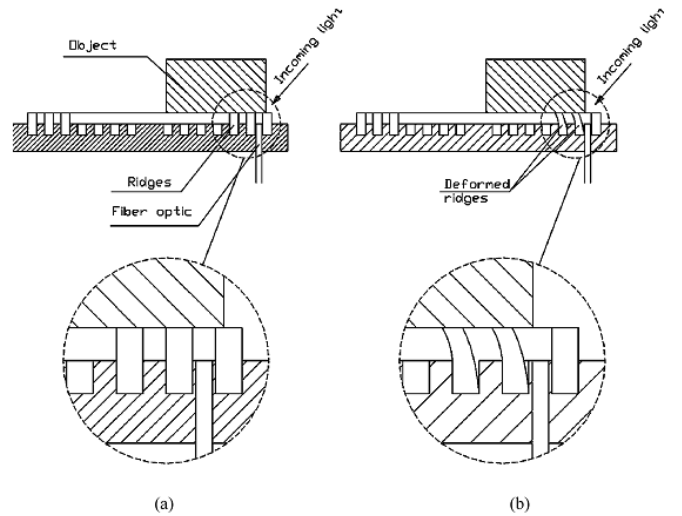


Fig. 9. Profile of optics-based tactile sensor illustrating effect of ridge deformation and principle of incipient slip detection, developed by William *et al.* When incipient slip occurs on the edge of the contact area, the relative displacement of the object to the sensor introduces light into the grooves between rubber ridges, which is captured by optic fibers. Reproduced from [85] with permission from Taylor & Francis (Copyright 2007).

from the eccentricity of the perimeter of the contact area, which is determined by processing an image captured from behind the transparent sensor surface.

Watanabe and Obinata [83] proposed an incipient slip sensor consisting of a CCD camera, LED lights, acrylic plate, and a spherical elastic body made of transparent silicone rubber patterned with a grid of dots (Fig. 8). The deformation of the elastic body (regions of incipient slip) are determined by analyzing the arrangement of the dots. The degree of slip was indicated by a “stick ratio” – the ratio of the area of incipient slip region to that of the contact region. The method was later improved to handle changes in slip direction or changes in the contact region area due to changes in the normal force [84].

William *et al.* [85] proposed a hemispherical tactile sensor with concentric circular ridges over its surface. The partial deformation of sensor ridges occurs on the edge of the contact area before gross slip, which is a measure of incipient slip. To detect the incipient slip, optic fibers are embedded into the grooves between rubber ridges (Fig. 9), and a change in

light intensity transmitted by those fibers is interpreted as an indication of incipient slip.

Tada and Hosoda [86] showed that it is possible to detect incipient slip from the vibrations they cause using PVDF films and strain gauges randomly embedded in a soft artificial fingertip. A NN was trained with the output of a camera to determine whether the grasped object had slipped or not. This work was extended in [87] – the output of a NN was used to control the grip force during object manipulation based on the PVDF and strain gauge signals from the sensor.

Mamun and Ibrahim [88] proposed a sensor that detects a local micro-displacement based on the mutual inductance property of an array of sensor elements. Each sensor element consists of three inductors: two of the inductors are stationary and carry alternating current, while the third inductor is short-circuited and mounted on a flexible rubber sheet placed between them. The sensing is achieved by detecting changes in mutual inductance as a function of the varying distance between a pair of inductors.

Ho and Hirai [89] proposed a soft semi-cylindrical rubber fingertip sensor with many uniformly distributed ridges on the outer (gripping) surface. Their results showed that during the transition from sticking to slipping, incipient slips occur on the contact line, propagating along the direction of slide. Instrumentation of the sensor has not yet been described.

In more recent work, Ho *et al.* [90] proposed modeling the human fingertip using virtual elastic compressible and bendable cantilevers and also created an artificial fingertip based on a sequence of magnetic resonance images of a human index finger. The bone and nail were 3-D printed, and the soft tissue was polyurethane rubber gel that had been cured in a mold. In agreement with observations made in the human finger [46], both the model and the artificial fingertip showed that incipient slips occur during tangential loading, initially near the boundary of the contact area, propagating from the periphery inward towards the center of contact. The ratio of slipped area to total contact area was used as a slip indicator (as in [83]) to control the grip force during a lifting simulation without needing to monitor the contact forces. Instrumentation of the artificial finger has not yet been described.

Yuan *et al.* [91] have proposed a novel method to measure incipient slip with a GelSight sensor, which consists of a clear elastomer coated with a reflective membrane with markers on its surface (Fig. 10(a) - (b)). When an object is pressed against the sensor, the elastomer deformation is recorded by a camera under illumination of colored lights. The displacement field of the elastomer is calculated by tracking the surface markers (Fig. 10(c) - (d)) and the entropy of the displacement field indicates the degree of incipient slip. The elastomer layer has since been given a curved surface [92], and recently a compact version of the sensor (GelSlim) has been described [93].

The sensors reviewed above detect incipient slip by measuring vibration, changes in stress and strain, deformation and displacement, using strain gauges, PVDF film, optical methods, inductance and force dependent resistances. However, those studies mainly consider incipient slip as an event detected by their system earlier than some external reference method of gross slip detection (e.g., using video, a potentiometer, or an

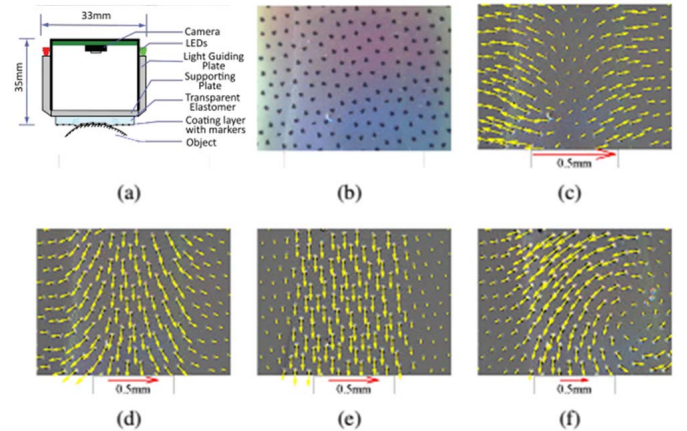


Fig. 10. GelSight sensor developed by Yuan *et al.* (a) Schematic, (b) camera view during grasping experiment with a soda can, (c) displacement field when grasping stably, (d) displacement field when the can is lifted stably, with shear field shown in (e) after subtracting the normal load displacement field of (c). (f) The response to an external torque on the can. Adapted from [91] with permission from IEEE (Copyright 2015).

optical linear encoder to measure the gross object displacement relative to the sensor). In our view, the validation of incipient slip detection requires a further step to determine the accuracy with which it can detect these events. Without that validation, there is a question whether the sensor is in fact detecting incipient slip, or whether it is simply able to detect the gross slip earlier than other traditional reference methods, which may be the case in [72], [85], and [86]. Only one of the works has attempted to validate the incipient slip detection itself [80], and a few works have validated the incipient slip detection against simulated results [74]–[76], [88]. That being said, a number of these works [74]–[77], [81], [83], [86], [91], [92] have attempted to integrate their sensors into some kind of gripping feedback control, which give a form of indirect validation.

D. Friction Estimation

To maintain a firm grip, most existing works ignore the need to sense the frictional properties of the SOI. There have been, however, a few works that have addressed this shortcoming in the literature by taking one of two approaches: (i) allowing gross or incipient slip to occur to determine friction; or (ii) estimating friction on contact with the object.

1) *Friction Estimation via Slip Detection:* A lab-based measurement of the static friction, μ_s , between two materials relies on measuring the tangential and normal forces at the moment of gross slip. Indeed, any gross slip detector could be combined with force sensing such that the tangential and normal forces are measured at the onset of gross slip to calculate μ_s . Furthermore, this could be performed either during an exploration of the object prior to manipulation, or during the manipulation itself, although in this latter case, there is a greater risk of dropping the object. One benefit of this approach is that during object manipulation, whenever a slip is detected, an updated estimate of μ_s can be determined. Alternatively, when used in conjunction with an incipient

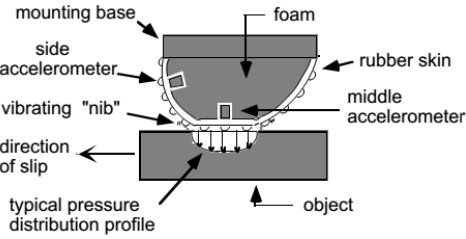


Fig. 11. Structure of the accelerometer-based artificial fingertip that detects incipient slip, developed by Tremblay and Cutkosky. The two accelerometers are used to detect slip-induced vibrations. The foam helps the fingertip conform to the grasped object surface to provide better grip, and reduces grip force control instability problems. The skin is covered with “nibs” that form local contact regions that can slip independently from one another and produce small vibrations when they do so. Reproduced from [95] with permission from IEEE (Copyright 1993).

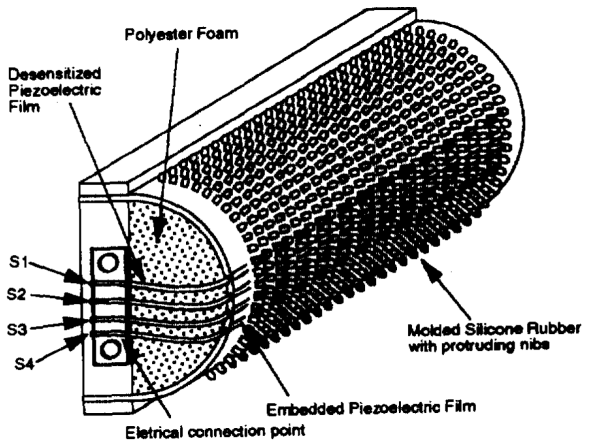


Fig. 12. The multi-element stress-rate sensor with slip detection capability, developed by Son *et al.* Reproduced from [96] with permission from IEEE (Copyright 1994).

slip detector, continuous force monitoring could provide an estimate of μ_s . If the global tangential-to-normal force ratio at the time of the incipient slip event is taken as an estimate of μ_s , it would generally be underestimated (which is better than obtaining an overestimate, from a grip security perspective) since the incipient slip would necessarily be in a region of the contact interface subject to a smaller normal force than the measured global normal force averaged over the contact area. A few reports are reviewed below that detect incipient slip with explicit reference to friction estimation.

Howe and Cutkosky [94] presented a slip sensor made of a thin textured rubber skin covering a soft inner layer of foam rubber, isolating the skin from structural vibrations in the manipulator. An accelerometer is attached to the inner surface of the skin to measure large local accelerations which are believed to be produced when areas of the skin catch and snap back as the sensor moves against a surface. Tremblay and Cutkosky [95] improved on this technique by moving the main accelerometer to the side of the fingertip for greater sensitivity to vibrations associated with incipient slips, and a second sensor was added at the center of the contact region (Fig. 11). Normal and tangential forces are also recorded via a three-axis force/torque sensor mounted behind the fingertip. An incipient slip is detected when a suprathreshold signal is present on the lateral accelerometer, but not on the accelerometer in the contact area, and the ratio of tangential-to-normal force at this time is taken as an estimate of μ_s .

Son *et al.* [96] describe a multi-element stress-rate sensor composed of four piezoelectric polymer strips molded into the surface of the rubber “skin” with protruding nibs (Fig. 12). Incipient slip can be detected by observing changes in two of the piezoelectric elements, which are measuring normal stress rate. An estimate of μ_s between the sensor and the manipulated object can be calculated by measuring the force signals just prior to the detected incipient slip.

Khamis *et al.* [97] recently proposed a proof-of-concept design for an incipient slip sensor which also estimates μ_s . The PapillArray is an array of silicone pillars with different uncompressed heights (Fig. 13). When compressed by a planar object surface, the tallest central pillars are under greater

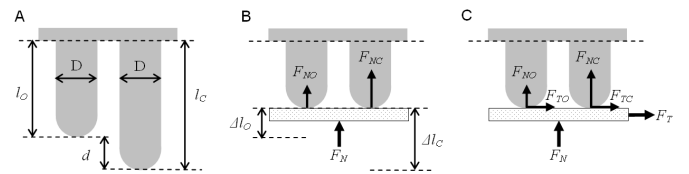


Fig. 13. The principle of operation of the PapillArray multi-pillar incipient slip sensor developed by Khamis *et al.* A central pillar and outer pillar of a PapillArray sensor, each with diameter D , and uncompressed heights l_C and l_O , respectively. The sensor is shown when A) it is uncompressed, B) it is compressed with a flat surface, and C) the surface is sheared. Reproduced from [97] with permission from Sensors & Actuators A (Copyright 2018).

normal stress and thus able to generate a greater friction force; this encourages the shorter outer pillars to slip first when a tangential force is applied. The incipient slip can be detected by measuring the deflection of the individual pillars. Also, when global forces are monitored, a simple mechanical model can be used to estimate μ_s each time an incipient slip is detected. Instrumentation for the PapillArray, to detect pillar slip, will be described in an upcoming publication.

In [94]–[96], there was no attempt to determine the relationship between the estimated μ_s and the actual μ_s . Only the PapillArray estimates of μ_s were validated against reference measurements of μ_s [97].

2) *Friction Estimation on Contact:* As an alternative to using gross slip detection and force measurement to estimate friction, a number of sensors have been proposed that measure μ_s when the sensor first contacts the object, but before there is any attempt to lift the object. In this scenario, slip still occurs when the object is first grasped, but it is in a symmetric fashion such that there is no relative gross movement between the sensor and the object. This approach incorporates the exploration procedure into the grasping action but, it does not typically allow further information on friction or grip security to be gathered during the manipulation task.

Nakamura and Shinoda [98], [99] proposed a tactile sensor using an acoustic resonance tensor cell (ARTC) sensing element, for estimating μ_s (Fig. 14). The ARTC is a parallelepiped cavity connected to an ultrasound transmitter and

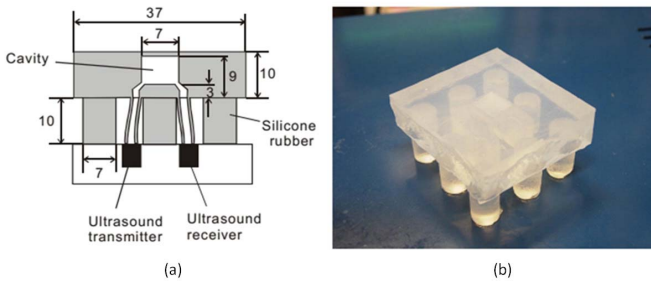


Fig. 14. Structure of the friction sensor developed by Nakamura and Shinoda: (a) schematic, and (b) sensor body made of transparent silicone rubber. The flat surface of the sensor makes contact with the object. Reproduced from [99] with permission from IEEE (Copyright 2001).

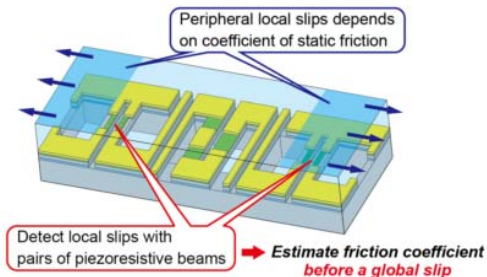


Fig. 15. Schematic of friction sensor developed by Okatani *et al.* – an elastomer embedded with three pairs of silicon beams with piezoresistors. The central pair of beams detect vertical strain, and the other two pairs detect lateral strain; both strains are dependent on the amount of incipient slip at the periphery of the contact area when a normal force compresses the elastomer. Reproduced from [102] with permission from MDPI (Copyright 2016).

receiver. From the three primary acoustic resonant frequencies of the cavity air, it detects the extension of the cavity along the edges (corresponding to vertical and horizontal strain), which should map to a value of μ_s according to the simulated results in [100] if well-calibrated.

Maeno *et al.* [101] proposed a method to estimate μ_s between a planar surface and an elastic finger sensor ([75], [76]; Fig. 6) on initial contact. The deformation of the elastic finger, the contact forces and the strain distribution were calculated from finite element analysis for various μ_s . Their results showed that shear strain differs with μ_s and can therefore be used to estimate friction.

Okatani *et al.* [102] describe a tactile sensor, composed of three pairs of parallel piezoresistive beams embedded in an elastomer (Fig. 15), which is able to measure normal and shear strains of the elastomer that are caused by applying a normal force. The relationship between normal and shear strains was found to be dependent on μ_s and it was proposed that this could be exploited to estimate μ_s .

Chen *et al.* [103], [104] proposed an eight-legged tactile sensor that can estimate μ_s between a planar surface and the sensor itself (Fig. 16). The sensor has eight (four pairs of) straight and rigid legs, each making a different predefined angle with respect to the vertical, which corresponds to a specified μ_s . A range including the exact value of μ_s can be estimated by simply determining how many sensor legs have slipped when pressed against a surface.

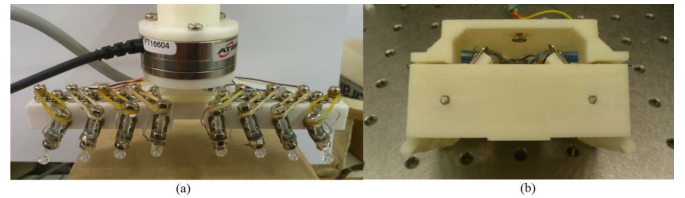


Fig. 16. Photos of (a) “spider” and (b) “spider2” sensors. Senses friction ranges by detecting which legs (arranged at different angles) slip when pressed against a planar object. Reproduced from [104] with permission from Springer, Copyright 2016.

The above sensors that propose measuring stress/strain in order to estimate μ_s at initial contact with an object, were able to show that the stress and strain distributions were dependent on μ_s ; however, most did not attempt to define a relationship between the measured quantities and μ_s [98], [99], [102]. A relationship between strain and μ_s was found in [101]; however, the range of μ_s for which the sensor was operational was severely limited ($\mu_s < 0.5$). Rather than providing an estimate of μ_s as a single value, the approach using rigid sensor legs [103], [104] provides an estimated range of μ_s . Increasing the number of legs (meaning more friction angles are tested) would increase the precision of the μ_s estimate; however, at present, the approach applies only to objects gripped on a planar surface, so extension to curved surfaces would be necessary in general.

IV. RECOMMENDATIONS

In the context of object manipulation, gross slip during manipulation is undesirable as it may lead to dropping the object. Therefore we consider gross slip detection as the last line of defense for grip security, and not generally suited as the only feedback regarding grip security.

In general, the type of information required during manipulation, and how often it is required, is application specific. Example applications for which a single estimate of friction at the onset of a manipulation task is sufficient include those where the environment is controlled and the friction with any one object is known to be constant. However, a sensor that gives a continuous indication of grip security (either by continuous measurement of friction, or by incipient slip detection, or both) would be more widely applicable and would likely facilitate superior dexterous manipulation. This is particularly important when the friction cannot be guaranteed to be constant throughout the manipulation task. This may be because the friction is nonlinearly dependent on normal force, contact area, and/or the rate of change of tangential force; e.g., silicone contacting a hard surface. Friction may also change during manipulation due to environmental factors; e.g., an outdoor application where rain water could form a fluid layer between the sensor and the gripped object.

A. Physical Design Considerations to Encourage Incipient Slip

1) *Technical Requirements:* For general manipulation scenarios, a sensor that detects incipient slip (either to estimate

friction or to indicate grip security without estimating friction) would be most suitable. The physical design of an incipient slip detection sensor must be conducive with allowing incipient slip to actually occur. The most direct design to ensure this is one in which the sensor surface consists of many individual components that can move independently of each other. The incipient slip sensor should also, by design, encourage incipient slip by ensuring that some individual components are more likely to slip than others under the same gross force conditions. This may be accounted for by the geometry (i.e., the relative sizes or orientations of individual moving components) of the sensor surface so that there is a pressure differential across the contact area. The mechanics of the sensor surface can also slow the incipient slip rate so it can be more easily detected.

2) *Challenges and Possible Solutions:* Yamada *et al.* [78] commented on the inability of their flat surface sensor to detect incipient slip and went on to say that in the curved surface case, the difference in pressure distribution across the contact area allows a peripheral sensor element to slip more easily and earlier than a central sensor element. They expanded on this by commenting that the radius of the curvature of the sensor surface is a critical parameter: too large and the normal contact force distributes too uniformly and the incipient slippage, once initiated, is not constrained to the edge of contact area and may be so widespread as to compromise the grip security; too small and the contact area is reduced and edges of the sensor are not in contact, even when a large normal force is applied [78].

The two most promising incipient slip sensors reported to date are the curved GelSight [92], and the PapillArray [97]. The dots on the soft elastomer of the GelSight sensor can move somewhat independently, and the curved surface encourages slip in some regions of the sensing surface more than any other, as the pressure profile is not uniform. Likewise, the pillars of the PapillArray sensor can move independently, and their differing uncompressed heights mean that shorter pillars are more likely to slip than taller pillars; however, an instrumentation method has not yet been proposed for measuring the displacement of the individual pillars in order to be able to practically detect incipient slip in real-time (this will appear in a future publication).

B. Instrumentation Considerations

1) *Technical Requirements:* In a sensor where many individual components move independently, detecting which components have slipped and which have not is a challenge and may require instrumentation of each component. The sensors reviewed in this paper have employed a number of different transduction techniques – resistive, inductive, piezoelectric, and optical – for measuring force and vibration and then analyzing these signals to estimate friction or detect incipient slip. Rather than a limited focus on forces and vibrations [105], [106], we suggest a focus on measuring displacement or stretch of the sensing surface, as this underpins measurement of friction on contact or detecting incipient slip (although transient events such as vibrations can help detect this too [107]).

2) *Challenges and Possible Solutions:* For measuring the displacements of many individual components in close proximity, a small sensing field down to the spacing of the individual components is required. A number of transduction techniques would not be suitable as it would be challenging to distinguish the source of the signal [108]. For example, signals from vibration sensitive transducers (e.g., PVDF film) are likely to be contaminated by vibrations from neighboring components, as well as vibrations due to gross movements of a gripper/arm in the context of robotic gripping. In such cases, additional analysis or decomposition of the vibration signal may be required to determine the source of the vibration. An optical transduction mechanism is more suitable, or alternatively, some electrical property could be measured, as optical and electrical isolation of individual sensing components are more easily achieved.

The goal of miniaturization must also be considered when selecting an instrumentation modality. Reducing the number of electrical components within the sensing area is desirable so as to not add to the sensor size and allow better manufacturability and access in the case of failing components. For example, Khamis *et al.* [109] use a lattice of conductive rubber strips and solve an underdetermined inverse problem to estimate surface deformation. This reduces the number of individual sensing elements and connecting wires, and eliminates the need for electronics within the sensing area. Optical instrumentation methods provide similar advantages in the context of slip sensors. Both the TacTip and GelSight/GelSlim sensors use a camera to track the displacement of pins or markers on the elastomer surface of the sensor and hence detect gross slip [61] or incipient slip [91]–[93]. The use of a camera, however, makes it challenging to develop a compact design [93] such as required for a skin. One solution is the incipient slip sensor proposed by William *et al.* [85], which uses optical fibers to detect changes in light intensity when a deformation occurs at the contact boundary indicating incipient slip.

C. Sensor Validation

It is important that incipient slip sensors and sensors that measure μ_s are properly validated. This involves comparing the incipient slip detections and/or friction estimates of the sensor to some external gold standard reference. Thus far, the sensors discussed here have been validated by performing gripping experiments that have focused on gripping objects with varying surface curvature, e.g., an object with a cylindrical or planar surface. However, progressing towards real-world application will require more thorough and general validation methods.

The performance of all the sensors reviewed here should be validated against surfaces with different geometries (e.g., planar, cylindrical, spherical), textures, and under different frictional conditions. This may prove particularly challenging for sensors that transduce vibration, as it is likely that vibration will be strongly dependent on some or all of these features. Also, sensor performance should also be validated against objects with hard surfaces as well as with surfaces that are softer than the sensor surface [77]. This is particularly

TABLE I

SUMMARY OF SENSORS REVIEWED. SENSOR PROPERTIES THAT ARE SUMMARIZED ARE: DIMENSIONS (WIDTH (W) × LENGTH (L) × HEIGHT (H) IN mm), WHERE WIDTH AND LENGTH REFER TO THE SENSOR FOOTPRINT, AND HEIGHT IS NORMAL TO THE GRIPPING SURFACE; TRANSDUCTION MECHANISM (E.G., VIBRATION, FORCE, STRAIN, DISPLACEMENT); METHOD OF INSTRUMENTATION (E.G., STRAIN GAUGE, PVDF); WHETHER THE DETECTION PARAMETER IS TRANSIENT (E.G., VIBRATION DUE TO A SLIP EVENT) OR PERSISTENT (E.G., STATIC STRAIN); SURFACE GEOMETRY; AND SURFACE MATERIAL. THE METHOD OF VALIDATING THE SENSOR, INCLUDING THE TESTS PERFORMED, THE OBJECTS AND CONDITIONS TESTED, AND THE REFERENCE AGAINST WHICH PERFORMANCE WAS MEASURED, AND THE REPORTED RESULTS ARE ALSO SUMMARIZED, AS WELL AS THE OVERALL ADVANTAGES AND DISADVANTAGES OF THE SENSOR. NR: NOT REPORTED

Sensor	W L H (mm)	Transduction mechanism; Instrumentation; Transient/persistent detection parameter	Surface geometry; Surface material	Validation method	Results	Advantages	Disadvantages
Gross Slip Detection							
[49]	0.8 10 0.1	Vibration; PVDF; Transient	Flat; Thin flexible Silicone	<i>Test:</i> Touching and rubbing sensor; <i>Objects/Conditions:</i> Finger; <i>Reference:</i> None.	Qualitative result: Sharp change of signals observed visually.		Vibration signal likely to be noisy during autonomous gripping.
[50], [51]	80 80 15	Vibration; Pressure sensitive resistors; Transient	Flat; Carbonized foam	<i>Test:</i> Induce gross slip between object and sensor; <i>Objects/Conditions:</i> 5 objects (4 flat, 1 curved), 2 normal forces (0.8 and 2 N); <i>Reference:</i> Position of robotic manipulator.	NN trained to estimate slipping velocity from frequency spectrum of sensor output; mean square error reported, but units are unclear.		Reference signal may not match actual slip velocity due to sensor compliance. NN must be trained on many shapes/surfaces. May not perform well for previously unseen surfaces.
[50], [52]				<i>Test:</i> Induce gross slip between object and two Myrmex sensors (one on either side of a gripper); <i>Objects/Conditions:</i> 3 objects, varying normal force (1 – 20 N); <i>Reference:</i> Onset of slip detected by evaluating contact forces.	NN trained to classify grip state from short-time Fourier transform of each of the 12×12 sensor cells of each of the two Myrmex sensors; 97% accuracy.		NN must be trained on shapes/surfaces. May not perform well for previously unseen surfaces.
[53]	16 40 20	Vibration; Strain gauges; Transient	Semi-cylindrical; Metal	<i>Test:</i> Induce gross slip between object and sensor; <i>Objects/Conditions:</i> Flat metal object; <i>Reference:</i> None.	Qualitative results: Reported good slip detection performance.		Hard sensor surface. Vibration signal likely to be noisy during autonomous gripping.
[54], [57]		Tangential force derivative; Impedance electrodes; Persistent		<i>Test:</i> Induce gross slip between object and sensor; <i>Objects/Conditions:</i> 3 objects with flat surfaces and 1 object with cylindrical surface (μ_s not specified); <i>Reference:</i> IMU for monitoring object motion.	Detects slip 18 ms ± 4.9 ms (plastic jar) and 4.7 ms ± 7.2 ms (wooden block) after IMU.		Detecting gross slip later than an IMU.
[55], [57]	15 28 14	Vibration; Pressure transducer; Transient		<i>Test:</i> Induce gross slip between object and sensor; <i>Objects/Conditions:</i> Multiple objects, multiple contact points, multiple slip speeds and directions; <i>Reference:</i> NR.	Detects slip 32.8 ms ± 4.2 ms (plastic jar) and 35.7 ms ± 6.0 ms (wooden block) before IMU.		Unclear if incipient slip detection or early gross slip detection – skin stretch may be insufficient for deformation required for incipient slip.
[56], [57]		Pressure, vibration, temperature; impedance electrodes, pressure transducer, temperature transducer; Persistent and transient	Anthropomorphic fingertip with fingerprint ridges; Elastomeric skin surrounding incompressible conductive fluid	<i>Test:</i> Grip stabilization (grip released until slip is predicted); <i>Objects/Conditions:</i> 7 objects (different weights, shapes and materials); <i>Reference:</i> NR.	Classifier to predict gross slip with 0.005, 0.01, 0.015, 0.02 s prediction horizon. Mean F score > 0.85 across all features for novel objects.	Comprehensive multimodal tactile sensor.	Longest prediction horizon of 0.02 s may not be sufficient for grip adjustment in the case of heavier objects or possibly in the presence of torque.
[56], [57]				<i>Test:</i> Induce gross slip between object and sensor and between object and external stylus (4 types of motion; 2 classes of slip); <i>Objects/Conditions:</i> 8 flat surfaces (different textures), 2 speeds (2 cm/s and ~5 cm/s); <i>Reference:</i> Type of slip known.	Stabilization success > 90% (0.02 s prediction horizon) for light objects. Stabilization success < 56% (0.02 s prediction horizon), for heavier objects.		
[56], [58], [59]	10 NR (each taxel)	Capacitance, vibration; Array of capacitive taxels, accelerometer; Persistent and transient	Flat with bumps with hemispherical ends; Silicone rubber	<i>Test:</i> Induce gross slip between object and sensor and between object and world (5 types of motion; 2 classes of slip); <i>Objects/Conditions:</i> 8 flat surfaces (different textures), 1 speed; <i>Reference:</i> Type of slip known.	Classification of slip condition: 89.6% accuracy using signal power (best frequency band), 75.9% accuracy using signal coherence (multiple fingers).		Can distinguish between 2 classes of slip (object/sensor slip and object world), but not concerned with slip onset.
[56]	25 31 NR	Vibration; PVDF; Transient	Curved with fingerprint ridges; Silicone rubber	<i>Test:</i> Induce gross slip between object and sensor and between object and world (2 types of motion, 2 classes of slip); <i>Objects/Conditions:</i> 3 flat surfaces (different textures), 2 contact forces (~5.5 N and ~10 N); <i>Reference:</i> Type of slip known.	Classification of slip condition: 87.4% accuracy using signal power (best frequency band), 100% accuracy using signal coherence (multiple fingers).		Shape encourages non-uniform pressure profile. Ridges may allow incipient slip without loss of grasp stability.
[61], [62]	40 40 NR	Displacement; Camera on backside; Transient	Hemi-spherical; Rubber skin and internal pins over gelatinous polymer blend	<i>Test:</i> Induce gross slip between object and sensor by slowly retracting sensor from a held object; <i>Objects/Conditions:</i> 4 objects with different curvatures; varying speed of slip onset; <i>Reference:</i> Position of held object relative to sensor.	Classification of slip condition: 99.88%.		With current materials, the skin stretch may be insufficient for deformation required for incipient slip.
Inciipient Slip Detection							
[71]	65 65 15	Ultrasonic vibration; PVDF; Transient	Hemi-spherical; Latex rubber on silicone rubber	<i>Test:</i> Induce gross slip between object and sensor; <i>Objects/Conditions:</i> One planar object; <i>Reference:</i> None.	Result of single test: slip generates acoustic emissions. Localization of source of emission presented but not validated.	Shape encourages non-uniform pressure profile.	Vibration signal likely to be noisy during autonomous gripping.
[72], [73]	20 20 NR	Centre of force distribution; Force dependent conductive rubber; Transient	Flat; Rubber	<i>Test:</i> Induce gross slip between object and sensor; <i>Objects/Conditions:</i> Multiple objects (details not reported); <i>Reference:</i> Potentiometer or robot joint position sensor to monitor object displacement.	Qualitative result: Slip detected with frequency analysis before potentiometer/joint position sensor.		Unclear if this is incipient slip detection or gross slip detection earlier than potentiometer/joint position sensor.
[74]- [76]	25 85 32.5	Strain; Strain gauges; Persistent	Semi-cylindrical; Silicone	<i>Test:</i> Induce gross slip between object and sensor; <i>Objects/Conditions:</i> Flat object, μ_s = 0.8 and 1.4; <i>Reference:</i> Finite element simulation.	Qualitative result: Distribution pattern of the strain is similar to finite element analysis.	Shape encourages non-uniform pressure profile.	Hardware is complex due to numerous sensors embedded in silicone rubber.
[77]	20 90 NR	Strain; Strain gauges; Transient	Semi-cylindrical with ridges; Silicone	<i>Test:</i> Grip force control; <i>Objects/Conditions:</i> Flat object, μ_s = 0.3 and 0.6; <i>Reference:</i> Finite element simulation.	Qualitative result: No gross slippage and no excessive normal force.		
[77]				<i>Test:</i> Induce gross slip between object and sensor; <i>Objects/Conditions:</i> Flat aluminum plate (μ_s not specified); <i>Reference:</i> None.	Result of single test: Impulse observed on second derivative of subtracted strain gauge pair signal, supposedly due to incipient slip.	Shape encourages non-uniform pressure profile.	
[79]	20 90 NR	Vibration; PVDF; Transient	Semi-cylindrical with ridges; Silicone	<i>Test:</i> Grasp force control – strategy unclear; <i>Objects/Conditions:</i> Rectangular parallelepiped shaped object with μ_s = 0.37, mass = 0.91 kg; <i>Reference:</i> None.	Result of single lift: Object whose weight and friction are unknown can be lifted without the occurrence of gross slip.	Shape encourages non-uniform pressure profile.	Hardware is complex due to numerous sensors embedded in silicone rubber.
[80]	NR	Normal and shear stress; PVDF; Persistent	Flat; Rubber	<i>Test:</i> Induce gross slip between object and sensor; <i>Objects/Conditions:</i> Multiple indenter shapes and sizes, multiple contact positions and force angles, and two friction limit angles; <i>Reference:</i> Traditional μ_s measurement.	Result of single test: Signals from one trial presented. Qualitative result: Incipient slip signal distinguishable from gripper movement.	Shape encourages non-uniform pressure profile.	
[81], [82]	NR	Shear deformation; Camera on backside; Persistent	Flat; Transparent acrylic	<i>Test:</i> Grip force control with slip margin target of 0.2 - load force applied, then doubled; <i>Objects/Conditions:</i> Hemi-spherical object, μ_s = 0.3 and 0.8; <i>Reference:</i> None.	NN trained to output tangential force/friction force (dimensionless); max error 0.222, mean error 0.047, S.D. 0.030.		NN must be trained on shapes/surfaces. Does not work for previously unseen surfaces.
[83]	NR	Displacement; Camera on backside; Persistent	Hemi-spherical; Elastic material	<i>Test:</i> Grip force control (proportional controller) with slip ratio (ratio of area slipping to entire contact area) target of 0.7; <i>Objects/Conditions:</i> Flat; <i>Reference:</i> Comparison with and without control.	Controller maintains target slip margin following a perturbation.	Shape encourages non-uniform pressure profile.	Limited to small deformations (i.e., small grip forces). Eccentricity of contact area as a measure of deformation is unlikely to work in the presence of torque.
					Qualitative result: slip occurs when no grip force control applied; with grip force control, slip does not occur, but target slip ratio not maintained (most likely due to proportional control strategy).	Shape encourages non-uniform pressure profile.	Limited to small deformations (i.e., small grip forces). Generalization of contact area threshold may be an issue.

TABLE I

(Continued.) SUMMARY OF SENSORS REVIEWED. SENSOR PROPERTIES THAT ARE SUMMARIZED ARE: DIMENSIONS (WIDTH (W) × LENGTH (L) × HEIGHT (H) IN mm), WHERE WIDTH AND LENGTH REFER TO THE SENSOR FOOTPRINT, AND HEIGHT IS NORMAL TO THE GRIPPING SURFACE; TRANSDUCTION MECHANISM (E.G., VIBRATION, FORCE, STRAIN, DISPLACEMENT); METHOD OF INSTRUMENTATION (E.G., STRAIN GAUGE, PVDF); WHETHER THE DETECTION PARAMETER IS TRANSIENT (E.G., VIBRATION DUE TO A SLIP EVENT) OR PERSISTENT (E.G., STATIC STRAIN); SURFACE GEOMETRY; AND SURFACE MATERIAL. THE METHOD OF VALIDATING THE SENSOR, INCLUDING THE TESTS PERFORMED, THE OBJECTS AND CONDITIONS TESTED, AND THE REFERENCE AGAINST WHICH PERFORMANCE WAS MEASURED, AND THE REPORTED RESULTS ARE ALSO SUMMARIZED, AS WELL AS THE OVERALL ADVANTAGES AND DISADVANTAGES OF THE SENSOR. NR: NOT REPORTED

[85]	50 50 NR	Displacement; Optic fiber; Persistent	Hemi-spherical with concentric ridges; Silicone rubber	<i>Test:</i> Induce gross slip between object and sensor; <i>Objects/Conditions:</i> Flat; <i>Reference:</i> Force derivative to indicate slip.	Qualitative result: Changes in light intensity on ridges near the contact boundary occur before a change in force is observed.	Shape encourages non-uniform pressure profile. Ridges may allow incipient slip without loss of grasp security. Easy to miniaturize.	Uncontrolled lighting conditions may pose a detection problem.
[86]	25 45 25	Vibration; PVDF and strain gauges; Transient	Anthropomorphic fingertip; Silicone	<i>Test:</i> Object lift and replace; <i>Objects/Conditions:</i> Two cups with different μ_s (μ_s not specified), five squares of timber with different weights (w_s , not specified); <i>Reference:</i> Vision system for monitoring object position.	NN trained with lift and replace experiments. During testing, slip is detected 180 ms earlier than the vision system.	Shape encourages non-uniform pressure profile.	Outputs of PVDF and strain gauges are noisy, with the latter prone to drift.
[87]	NR	Vibration; PVDF and strain gauges; Transient	Anthropomorphic fingertip; Silicone	<i>Test:</i> Grip force control; <i>Objects/Conditions:</i> Cylindrical object made from plastic, containing water (150 g and 450 g, μ_s not specified); <i>Reference:</i> None.	Qualitative result: Signals from one trial (150 g object) presented. Pneumatic pressure (grip strength) compared for 150 g and 450 g object.		
[88]	NR	Displacement; Inductors; Persistent	Flat; Rubber with protruding contact points	<i>Test:</i> Simulation with a primary coil and two secondary coils; <i>Objects/Conditions:</i> N/A; <i>Reference:</i> Simulation.	Results of simulation: Displacement can be detected.	Independent contact points may allow incipient slip without loss of grasp stability.	
[89]	3 10 NR	Displacement; N/A; Persistent	Semi-cylindrical with parallel ridges; Rubber	<i>Test:</i> Induce gross slip between object and sensor, and image tracking through transparent object; <i>Objects/Conditions:</i> Transparent rigid plane; <i>Reference:</i> None.	Results of single trial: Image tracking through transparent rigid plane shows cascade of incipient slip of ridges before all ridges are slipping.	Shape encourages non-uniform pressure profile. Ridges allow incipient slip without loss of grasp stability.	Instrumentation not yet described. Incipient slip can only be detected along direction normal to the length of the ridges.
[90]	NR NR NR	Displacement; N/A; Persistent	Anthropomorphic fingertip; Polyurethane rubber	<i>Test:</i> Induce gross slip between object and sensor, and image tracking through transparent object; <i>Objects/Conditions:</i> Transparent rigid plane; <i>Reference:</i> Simulation.	Results of single trial: Image tracking through transparent rigid plane shows cascade of incipient slip (localized displacements). Experimental results align with simulation results.	Shape encourages non-uniform pressure profile.	Instrumentation not yet described.
[91]	33 33 35	Displacement; Camera on backside;	Flat; Elastomer gel with dots marked	<i>Test:</i> Induce gross slip between object and sensor; <i>Objects/Conditions:</i> Indenters with different sizes and shapes (flat and cylindrical); <i>Reference:</i> None.	Shear field entropy of displacement of dots increases as tangential load increases.	Material allows large deformation allowing incipient slip without loss of grasp security.	Very long settling time to reach quasi-static state. Range of shear field entropy that indicates incipient slip differs for different shape indenters – unclear if this is dependent on friction. Softness of elastomer may present problems with wear and require frequent replacement.
[92]	35 35 35	Persistent	Curved; Elastomer gel with dots marked	<i>Test:</i> Grip force control; <i>Objects/Conditions:</i> Multiple object (beer can, pen, key, spoon, USB flash drive); <i>Reference:</i> None.	Qualitative result: Displacement field of surface markers effectively represent contact condition of sensor and object.	Shape encourages non-uniform pressure profile.	Issues of settling time and range of shear field entropy not addressed. Softness of elastomer may present problems with wear and require frequent replacement.
Friction Measurement (on slip)							
[94],[95]	NR	Acceleration; Accelerometer; Transient	Hemi-spherical with nibs; Rubber skin surrounding rubber foam	<i>Test:</i> Induce gross slip between object and sensor; <i>Objects/Conditions:</i> Flat object covered with photocopy paper; <i>Reference:</i> Accelerometer indicating relative movement of object/sensor.	Qualitative results: In most cases, significant sensor output begins 40–100 ms before the platform has moved 1 mm.	Shape encourages non-uniform pressure profile. Nibs may allow incipient slip without loss of grasp security.	Large signals present when gripper moving.
[96]	25 45 25	Normal stress rate; Piezoelectric polymer strips; Transient	Semi-cylindrical with nibs; Silicone rubber on polyester foam	<i>Test:</i> Grip force control (decrease grip force and double load force); <i>Objects/Conditions:</i> Flat object covered in fine grain sandpaper, 2 N normal force; <i>Reference:</i> Accelerometer and optical encoder indicating relative movement of object/sensor.	Qualitative results: Response of gripper to incipient slip presented, but no validation of calculated friction, does not compare to case of no control, does not test multiple objects/frictions.		
[97]	80 80 15	Displacement; N/A; Persistent	Pillars with hemispherical tips and different heights; Silicone	<i>Test:</i> Induce gross slip between object and sensor and image tracking through transparent object; <i>Objects/Conditions:</i> Transparent flat acrylic (3 frictions), 5, 7.5, 10, 12.5 and 15 N normal force; <i>Reference:</i> Traditional measurement of μ_s .	Results of single trial: Signals from two of the sensors begin to change 95 and 47 ms earlier than relative motion.	Shape encourages non-uniform pressure profile. Nibs may allow incipient slip without loss of grasp security.	Incipient slip signals are much smaller than signals from contact events - slip detection during autonomous manipulation difficult.
[98]	80 80 15	Displacement; N/A; Persistent	Pillars with hemispherical tips and different heights; Silicone	<i>Test:</i> Induce gross slip between object and sensor and image tracking through transparent object; <i>Objects/Conditions:</i> Transparent flat acrylic (3 frictions), 5, 7.5, 10, 12.5 and 15 N normal force; <i>Reference:</i> Traditional measurement of μ_s .	Estimated μ_s vs. actual μ_s (measured with traditional procedure): $R^2 = 0.95$.	Shape encourages non-uniform pressure profile; Independently moving pillars allow incipient slip without loss of grasp security.	Instrumentation for measuring pillar displacement not yet described. Current estimate of μ_s dependent on contact with planar object.
Friction Measurement (on contact)							
[100]	37 37 20	Vertical and horizontal strain; Ultrasound; Persistent	Flat; Silicone rubber	<i>Test:</i> Normal contact; <i>Objects/Conditions:</i> Multiple frictions, inclines, contact speeds, shapes (flat and curved); <i>Reference:</i> N/A.	Difference in ratio of vertical to horizontal extension for friction and negligible effect due to inclines contact speeds and shapes (except the effect on settling time).		Long settling times (on the order of tens of seconds).
[75], [76], [101]	20 36.6	Shear strain; Strain gauges; Persistent	Semi-cylindrical; Silicone	<i>Test:</i> Normal contact; <i>Objects/Conditions:</i> 7 objects with μ_s between 0.3 and 0.55; <i>Reference:</i> Traditional measurement of μ_s .	Second order relationship between the strain and μ_s could be approximated which enables μ_s to be estimated with an accuracy of 0.1. Unsatisfactory repeatability for $\mu_s > 0.5$.	Shape encourages non-uniform pressure profile.	Limited range of μ_s (< 0.5) severely limits usefulness. Strain distribution curves for different μ_s are not well separated, which will result in poor resolution.
[102]	11 11 2	Vertical and lateral strain; 3 pairs of piezoresistive beams; Persistent	Flat; Elastomer	<i>Test:</i> Normal contact; <i>Objects/Conditions:</i> Flat acrylic plate coated with talcum powder, $\mu_s = 0.2, 0.4, 0.8$ and 1.1; <i>Reference:</i> Simulation and traditional μ_s measurement.	Measured vertical and lateral strains matched simulation. Qualitative result: Relationship between fractional resistance changes corresponding to vertical and lateral strains is dependent on μ_s .		
[103]	150 40 42.8	Displacement; Contact switches; Persistent	Flat; Rigid legs on hinges	<i>Test:</i> Normal contact; <i>Objects/Conditions:</i> 5 flat surfaces with $\mu_s = 0.08 – 0.5$; <i>Reference:</i> Traditional measurement of μ_s .	Estimated μ_s vs. actual μ_s (measured with traditional procedure): $R^2 = 0.924$.	More legs (at more angles) can be added for better quantization of μ_s . Potential for to miniaturization.	Requires baseline normal force to overcome restorative elastic forces on legs.
[104]	72 51.2 42.6	Displacement; Contact switches; Persistent	Flat; Rigid legs on hinges	<i>Test:</i> Normal contact; <i>Objects/Conditions:</i> 9 flat surfaces with $\mu_s = 0.13 – 0.76$; <i>Reference:</i> Traditional measurement of μ_s .	Estimated μ_s vs. actual μ_s (measured with traditional procedure): $R^2 = 0.918$.		Requires planar object to ensure angles between legs and object are known (may be solved with miniaturization).

important for grip security sensors made of a soft/deformable material as this will undoubtedly affect the deformation of the sensor surface and may limit the sensors sensing ability.

D. Considerations for Use With Grip-Force Control Systems

1) *Torque*: A tactile sensor which measures aspects of grip security (force, friction, slip, etc.) is part of a larger system containing a gripper and gripper control system, as well as a robotic or prosthetic arm governed by another control system. While it is not necessary to measure contact forces to detect slip events, monitoring the contact forces and torques is still required in order to either estimate friction, or to indicate and monitor the magnitude of grip force adjustment required to prevent further incipient slip; the grip force must counter both tangential load and torque which may arise when an object is gripped in a location that does not pass through its center of mass. Thus far, most studies of incipient slip have considered only linear motions. An important future consideration is to also validate these sensors under rotations, and it remains an open question which existing sensors would function well in the presence of torque.

2) *Resetting Sensor Configuration*: Finally, for incipient slip sensors, some consideration needs to be made with respect to how these sensors are to recover to their original configuration after incipient slip and grip force adjustment. In some cases, the components that have already slipped will be unable to signal any future incipient slip and therefore future function of the sensor may be compromised and the sensor can no longer indicate incipient slip across the entire sensor surface. This may mean that once a grip force adjustment is made, any new incipient slip must be treated much more conservatively, and a decision may even be required to replace the object so that it can be lifted again with the sensor in its original configuration. Alternatively, a multi-fingered hand may be employed so that one of the fingers/sensors can break and then remake contact with the object in its original configuration while the other fingers maintain the grasp. Slip detection that relies on transient signals e.g., shear velocity, may be more robust to pre-deformation of the sensor surface. As far as we are aware no existing study has considered this, and yet it is clearly an aspect of human touch as we are able feel slip no matter how the fingertip is pre-deformed before slippage.

V. CONCLUSION

Tactile sensing is essential for improving robotic and prosthetic gripping performance in unstructured environments. Friction is a critical factor determining the grasp stability of certain grip poses. Therefore, measuring friction, or friction-dependent mechanical events such as gross and incipient slip, is particularly important in the context of stable gripping. Combined with measured contact forces and torques, knowledge of friction enables a more precise estimation of the minimum grip force required to securely grasp an object.

Measuring friction during an exploratory task before attempting to grip an object, or measuring friction on contact, is not practical as friction may not be constant. Furthermore, allowing gross slip to occur during a manipulation task in

order to measure friction means there is a high risk of dropping the object. If a friction measurement is performed on contact, or following an incipient slip event, then a controlled slip is required. Achieving this is dependent on the geometry of the sensor surface and mechanical properties of the sensor material. The optimal geometry allows relatively independent movement, so that part of the sensor surface can slip while another part remains stuck to the object, and it encourages slip in some parts more than others by varying contact pressure/force across the sensor/gripping surface.

Detecting incipient slip events with sensors remains a challenge. During dexterous manipulation, humans seem to use vibration and strain to sense incipient slip in the glabrous skin on the fingers and palm. In robotic systems however, the small vibrations due to the incipient slip events are often masked by large vibrations caused by the motors and gross movements in the system. The most promising methods of instrumentation to date all rely on optics to measure displacement on the sensor/gripping surface, however further work is still required to develop a state-of-the art friction/grip security sensor that functions comparably to the human hand.

In our view, dexterous object manipulation is a difficult challenge, but the ultimate solution will undoubtedly involve a confluence of state-of-the-art advancements in position-and force-feedback-controlled robotics, machine vision, multimodal sensor fusion, artificial intelligence, and of course, tactile sensing. The authors strongly believe that future developments of tactile sensors which sense friction or can reliably sense incipient slip, inspired by the human finger, will propel the functionality of tactile sensing to a point where dexterous object manipulation on par with human performance becomes a feasible prospect. We hope that the articles compiled in this review, and the recommendations proposed, will help us reach this goal.

REFERENCES

- [1] Å. B. Vallbo and R. S. Johansson, "Properties of cutaneous mechanoreceptors in the human hand related to touch sensation," *Human Neurobiol.*, vol. 3, no. 1, pp. 3–14, 1984.
- [2] V. G. Macfield and I. Birznieks, "Cutaneous mechanoreceptors, functional behavior," in *Encyclopedia of Neuroscience*, M. D. Binder, N. Hirokawa, and U. Windhorst, Eds. Berlin, Germany: Springer, 2009, pp. 914–922.
- [3] A. W. Goodwin, P. Jenmalm, and R. S. Johansson, "Control of grip force when tilting objects: Effect of curvature of grasped surfaces and applied tangential torque," *J. Neurosci.*, vol. 18, no. 24, pp. 10724–10734, 1998.
- [4] I. Birznieks, P. Jenmalm, A. W. Goodwin, and R. S. Johansson, "Encoding of direction of fingertip forces by human tactile afferents," *J. Neurosci.*, vol. 21, no. 20, pp. 8222–8237, 2001.
- [5] I. Birznieks, H. E. Wheat, S. J. Redmond, L. M. Salo, N. H. Lovell, and A. W. Goodwin, "Encoding of tangential torque in responses of tactile afferent fibres innervating the fingerpad of the monkey," *J. Physiol.*, vol. 588, pp. 1057–1072, Apr. 2010.
- [6] A.-S. Augurelle, A. M. Smith, T. Lejeune, and J.-L. Thonnard, "Importance of cutaneous feedback in maintaining a secure grip during manipulation of hand-held objects," *J. Neurophysiol.*, vol. 89, pp. 665–671, Feb. 2003.
- [7] R. S. Johansson and G. Westling, "Roles of glabrous skin receptors and sensorimotor memory in automatic control of precision grip when lifting rougher or more slippery objects," *Exp. Brain Res.*, vol. 56, no. 3, pp. 550–564, 1984.
- [8] G. Westling and R. S. Johansson, "Factors influencing the force control during precision grip," *Exp. Brain Res.*, vol. 53, no. 2, pp. 277–284, 1984.

- [9] J. Tegin and J. Wikander, "Tactile sensing in intelligent robotic manipulation—A review," *Ind. Robot. Int. J.*, vol. 32, no. 1, pp. 64–70, Feb. 2005.
- [10] M. I. Tiwana, S. J. Redmond, and N. H. Lovell, "A review of tactile sensing technologies with applications in biomedical engineering," *Sens. Actuators A, Phys.*, vol. 179, pp. 17–31, Jun. 2012.
- [11] R. Bayreithner and K. Komoriya, "Static friction coefficient determination by force sensing and its application," in *Proc. IEEE/RSJ/GI Int. Conf. Intell. Robots Syst., Adv. Robot. Syst. Real World*, Sep. 1994, pp. 1639–1646.
- [12] A. Bicchi, "Intrinsic contact sensing for soft fingers," in *Proc. IEEE Int. Conf. Robot. Automat.*, May 1990, pp. 968–973.
- [13] B. Bhushan, *Introduction to Tribology*. Hoboken, NJ, USA: Wiley, 2013.
- [14] M. J. Adams *et al.*, "Finger pad friction and its role in grip and touch," *J. Roy. Soc. Interface*, vol. 10, no. 80, p. 20120467, 2013.
- [15] S. M. Pasumarty, S. A. Johnson, S. A. Watson, and M. J. Adams, "Friction of the human finger pad: Influence of moisture, occlusion and velocity," *Tribol. Lett.*, vol. 44, p. 117, Nov. 2011.
- [16] A. Ruina and J. R. Rice, "Stability of steady frictional slipping," *J. Appl. Mech.*, vol. 50, no. 2, pp. 343–349, Jun. 1983.
- [17] O. Ben-David, G. Cohen, and J. Fineberg, "The dynamics of the onset of frictional slip," *Science*, vol. 330, no. 6001, pp. 211–214, 2010.
- [18] O. M. Braun, I. Barel, and M. Urbakh, "Dynamics of transition from static to kinetic friction," *Phys. Rev. Lett.*, vol. 103, p. 194301, Nov. 2009.
- [19] S. M. Rubinstein, G. Cohen, and J. Fineberg, "Detachment fronts and the onset of dynamic friction," *Nature*, vol. 430, pp. 1005–1009, Aug. 2004.
- [20] R. S. Dahiya, G. Metta, M. Valle, and G. Sandini, "Tactile sensing—From humans to humanoids," *IEEE Trans. Robot.*, vol. 26, no. 1, pp. 1–20, Feb. 2010.
- [21] P. S. Girão, P. M. P. Ramos, O. Postolache, and J. M. D. Pereira, "Tactile sensors for robotic applications," *Measurement*, vol. 46, no. 3, pp. 1257–1271, 2013.
- [22] R. D. Howe, "Tactile sensing and control of robotic manipulation," *Adv. Robot.*, vol. 8, no. 3, pp. 245–261, 1993.
- [23] D. Javad and N. Siamak, "Advances in tactile sensors design/manufacturing and its impact on robotics applications—A review," *Ind. Robot. Int. J.*, vol. 32, no. 3, pp. 268–281, 2005.
- [24] M. H. Lee and H. R. Nicholls, "Review article tactile sensing for mechatronics—A state of the art survey," *Mechatronics*, vol. 9, no. 1, pp. 1–31, 1999.
- [25] H. Yousef, M. Boukallel, and K. Althoefer, "Tactile sensing for dexterous in-hand manipulation in robotics—A review," *Sens. Actuators A, Phys.*, vol. 167, no. 2, pp. 171–187, 2011.
- [26] Z. Kappassov, J.-A. Corrales, and V. Perdereau, "Tactile sensing in dexterous robot hands—Review," *Robot. Auton. Syst.*, vol. 74, pp. 195–220, Dec. 2015.
- [27] H. P. Saal and S. J. Bensmaia, "Touch is a team effort: Interplay of submodalities in cutaneous sensibility," *Trends Neurosci.*, vol. 37, no. 12, pp. 689–697, 2014.
- [28] H. Khamis, I. Birznieks, and S. J. Redmond, "Decoding tactile afferent activity to obtain an estimate of instantaneous force and torque applied to the fingerpad," *J. Neurophysiol.*, vol. 114, no. 1, pp. 474–484, 2015.
- [29] H. A. Khamis, S. J. Redmond, V. G. Macefield, and I. Birznieks, "Tactile afferents encode grip safety before slip for different frictions," in *Proc. 36th Annu. Int. Conf. IEEE Eng. Med. Biol. Soc. (EMBC)*, Aug. 2014, pp. 4123–4126.
- [30] S. Derler and L.-C. Gerhardt, "Tribology of skin: Review and analysis of experimental results for the friction coefficient of human skin," *Tribol. Lett.*, vol. 45, no. 1, pp. 1–27, 2012.
- [31] F. M. Hendriks, D. V. Brokken, J. T. van Eemeren, C. W. Oomens, F. P. Baaijens, and J. B. Horsten, "A numerical-experimental method to characterize the non-linear mechanical behaviour of human skin," *Skin Res. Technol.*, vol. 9, no. 3, pp. 274–283, 2003.
- [32] J. E. Bischoff, E. M. Arruda, and K. Grosh, "Finite element modeling of human skin using an isotropic, nonlinear elastic constitutive model," *J. Biomech.*, vol. 33, no. 6, pp. 645–652, 2000.
- [33] O. S. Dinç, C. M. Ettles, S. J. Calabrese, and H. A. Scarton, "Some parameters affecting tactile friction," *J. Tribol.*, vol. 113, no. 3, pp. 512–517, 1991.
- [34] P. H. Warman and A. R. Ennos, "Fingerprints are unlikely to increase the friction of primate fingerpads," *J. Exp. Biol.*, vol. 212, no. 13, pp. 2016–2022, 2009.
- [35] J. Scheibert, S. Leurent, A. Prevost, and G. Debrégeas, "The role of fingerprints in the coding of tactile information probed with a biomimetic sensor," *Science*, vol. 323, no. 5920, pp. 1503–1506, 2009.
- [36] L. Cramphorn, B. Ward-Cherrier, and N. F. Lepora, "Addition of a biomimetic fingerprint on an artificial fingertip enhances tactile spatial acuity," *IEEE Robot. Autom. Lett.*, vol. 2, no. 3, pp. 1336–1343, Jul. 2017.
- [37] T. André, P. Lefèvre, and J. L. Thonnard, "Fingertip moisture is optimally modulated during object manipulation," *J. Neurophysiol.*, vol. 103, no. 1, pp. 402–408, 2010.
- [38] G. Cadoret and A. M. Smith, "Friction, not texture, dictates grip forces used during object manipulation," *J. Neurophysiol.*, vol. 75, pp. 1963–1969, May 1996.
- [39] R. S. Johansson and G. Westling, "Influences of cutaneous sensory input on the motor coordination during precision manipulation," in *Somatosensory Mechanisms*, C. von Euler, O. Franzén, U. Lindblom, and D. Ottoson, Eds. London, U.K.: Palgrave Macmillan, 1984, pp. 249–260.
- [40] R. S. Johansson and J. R. Flanagan, "Coding and use of tactile signals from the fingertips in object manipulation tasks," *Nature Rev. Neurosci.*, vol. 10, no. 5, pp. 345–359, 2009.
- [41] R. S. Johansson and G. Westling, "Signals in tactile afferents from the fingers eliciting adaptive motor responses during precision grip," *Exp. Brain Res.*, vol. 66, no. 1, pp. 141–154, 1987.
- [42] H. Khamis, S. J. Redmond, V. Macefield, and I. Birznieks, "Classification of texture and frictional condition at initial contact by tactile afferent responses," in *Proc. Int. Conf. Hum. Haptic Sens. Touch Enabled Comput. Appl.*, 2014, pp. 460–468.
- [43] S. A. Johnson, D. M. Gorman, M. J. Adams, and B. J. Briscoe, "The friction and lubrication of human stratum corneum," in *Proc. 19th Leeds-Lyon Symp. Tribol.*, Inst. Tribology, Univ. Leeds, Leeds, U.K., vol. 25, D. Dowson *et al.*, Eds. Amsterdam, The Netherlands: Elsevier, 1993, pp. 663–672.
- [44] S. E. Tomlinson, R. Lewis, and M. J. Carré, "Review of the frictional properties of finger-object contact when gripping," *Proc. Inst. Mech. Eng., J. J. Eng. Tribol.*, vol. 221, no. 8, pp. 841–850, 2007.
- [45] B. Dzidek, S. Bochereau, S. A. Johnson, V. Hayward, and M. J. Adams, "Why pens have rubbery grips," *Proc. Nat. Acad. Sci. USA*, vol. 114, no. 41, pp. 10864–10869, 2017.
- [46] B. Delhayé, P. Lefèvre, and J.-L. Thonnard, "Dynamics of fingertip contact during the onset of tangential slip," *J. Roy. Soc. Interface*, vol. 11, no. 100, p. 20140698, 2014.
- [47] Q. Wang and V. Hayward, "In vivo biomechanics of the fingerpad skin under local tangential traction," *J. Biomechanics*, vol. 40, no. 4, pp. 851–860, 2007.
- [48] M. T. Francomano, D. Accoto, and E. Guglielmelli, "Artificial sense of slip—A review," *IEEE Sensors J.*, vol. 13, no. 7, pp. 2489–2498, Jul. 2013.
- [49] B. Choi, H. R. Choi, and S. Kang, "Development of tactile sensor for detecting contact force and slip," in *Proc. IEEE/RSJ Int. Conf. Intell. Robots Syst.*, Aug. 2005, pp. 2638–2643.
- [50] C. Schüermann, R. Haschke, H. Ritter, and A. Citec, "Modular high speed tactile sensor system with video interface," in *Proc. Tactile Sens. Humanoids-Tactile Sensors Beyond IEEE-RAS Conf. Humanoid Robots (Humanoids)*, Paris, France, 2009, pp. 524–527.
- [51] M. Schöepfer, C. Schüermann, M. Pardowitz, and H. Ritter, "Using a piezo-resistive tactile sensor for detection of incipient slip-page," in *Proc. 41st Int. Symp. Robot. (ISR), 6th German Conf. Robot. (ROBOTIK)*, 2010, pp. 1–7.
- [52] M. Meier, F. Patzelt, R. Haschke, and H. J. Ritter, "Tactile convolutional networks for online slip and rotation detection," in *Proc. Int. Conf. Artif. Neural Netw.*, 2016, pp. 12–19.
- [53] R. Fernandez, I. Payo, A. S. Vazquez, and J. Becedas, "Micro-vibration-based slip detection in tactile force sensors," *Sensors*, vol. 14, pp. 709–730, Jan. 2014.
- [54] Z. Su *et al.*, "Force estimation and slip detection/classification for grip control using a biomimetic tactile sensor," in *Proc. IEEE-RAS 15th Int. Conf. Humanoid Robots (Humanoids)*, Nov. 2015, pp. 297–303.
- [55] F. Veiga, J. Peters, and T. Hermans, "Grip stabilization of novel objects using slip prediction," *IEEE Trans. Haptics*, to be published. [Online]. Available: <http://ieeexplore.ieee.org/stamp/stamp.jsp?tp=&arnumber=8361482&isnumber=4543166>, doi: 10.1109/TOH.2018.2837744.
- [56] B. Heyneman and M. R. Cutkosky, "Slip classification for dynamic tactile array sensors," *Int. J. Robot. Res.*, vol. 35, no. 4, pp. 404–421, 2016.

- [57] M. C. Jimenez and J. A. Fishel, "Evaluation of force, vibration and thermal tactile feedback in prosthetic limbs," in *Proc. IEEE Haptics Symp.*, Feb. 2014, pp. 437–441.
- [58] B. Heyneman and M. R. Cutkosky, "Biologically inspired tactile classification of object-hand and object-world interactions," in *Proc. IEEE Int. Conf. Robot. Biomimetics (ROBIO)*, Dec. 2012, pp. 167–173.
- [59] D. M. Aukes *et al.*, "Design and testing of a selectively compliant underactuated hand," *Int. J. Robot. Res.*, vol. 33, no. 5, pp. 721–735, 2014.
- [60] K. Van Wyk and J. Falco, "Calibration and analysis of tactile sensors as slip detectors," presented at the Int. Conf. Robot. Automat. (ICRA), Brisbane, QLD, Australia, May 21–25, 2018.
- [61] J. W. James, N. Pestell, and N. F. Lepora, "Slip detection with a biomimetic tactile sensor," *IEEE Robot. Autom. Lett.*, vol. 3, no. 4, pp. 3340–3346, Oct. 2018.
- [62] C. Chorley, C. Melhuish, T. Pipe, and J. Rossiter, "Development of a tactile sensor based on biologically inspired edge encoding," in *Proc. Int. Conf. Adv. Robot.*, 2009, pp. 1–6.
- [63] D. Goeger, N. Ecker, and H. Woern, "Tactile sensor and algorithm to detect slip in robot grasping processes," in *Proc. IEEE Int. Conf. Robot. Biomimetics*, Feb. 2009, pp. 1480–1485.
- [64] D. Gunji *et al.*, "Grasping force control of multi-fingered robot hand based on slip detection using tactile sensor," in *Proc. IEEE Int. Conf. Robot. Automat.*, May 2008, pp. 2605–2610.
- [65] M. I. Tiwanaa, A. Shashankb, S. J. Redmond, and N. H. Lovell, "Characterization of a capacitive tactile shear sensor for application in robotic and upper limb prostheses," *Sens. Actuators A, Phys.*, vol. 165, no. 2, pp. 164–172, 2011.
- [66] B. B. Edin, L. Ascari, L. Beccai, S. Roccella, J.-J. Cabibihan, and M. C. Carrozza, "Bio-inspired sensorization of a biomechatronic robot hand for the grasp-and-lift task," *Brain Res. Bull.*, vol. 75, no. 6, pp. 785–795, Apr. 2008.
- [67] B. Yang, X. Duan, and H. Deng, "A simple method for slip detection of prosthetic hand," in *Proc. IEEE Int. Conf. Inf. Automat.*, Aug. 2015, pp. 2159–2164.
- [68] C. Pasluosta, H. Tims, and L. Chiu, "Slippage sensory feedback and nonlinear force control system for a low-cost prosthetic hand," *Amer. J. Biomed. Sci.*, vol. 1, no. 4, pp. 295–302, 2009.
- [69] Y. Liu, H. Han, T. Liu, J. Yi, Q. Li, and Y. Inoue, "A novel tactile sensor with electromagnetic induction and its application on stick-slip interaction detection," *Sensors*, vol. 16, no. 4, p. 430, 2016.
- [70] D. Dornfeld and C. Handy, "Slip detection using acoustic emission signal analysis," in *Proc. IEEE Int. Conf. Robot. Automat.*, Mar./Apr. 1987, pp. 1868–1875.
- [71] S. Ando and H. Shinoda, "Ultrasonic emission tactile sensing," *IEEE Control Syst. Mag.*, vol. 15, no. 1, pp. 61–69, Feb. 1995.
- [72] L. Marconi and C. Melchiorri, "Incipient slip detection and control using a rubber-based tactile sensor," in *Proc. IFAC World Congr.*, 1996, pp. 475–480.
- [73] E. G. M. Holweg, H. Hoeve, W. Jongkind, L. Marconi, C. Melchiorri, and C. Bonivento, "Slip detection by tactile sensors: Algorithms and experimental results," in *Proc. IEEE Int. Conf. Robot. Automat.*, Apr. 1996, pp. 3234–3239.
- [74] T. Maeno, K. Kobayashi, and N. Yamazaki, "Sensing mechanisms of the partial incipient slip at the surface of cylindrical fingers during the precision grip," in *Proc. ASME Summer Bioeng. Conf.*, 1997, pp. 117–118.
- [75] T. Maeno, T. Kawai, and K. Kobayashi, "Analysis and design of a tactile sensor detecting strain distribution inside an elastic finger," in *Proc. IEEE/RSJ Int. Conf. Intell. Robots Syst.*, Oct. 1998, pp. 1658–1663.
- [76] T. Maeno, S. Hiromitsu, and T. Kawai, "Control of grasping force by detecting stick/slip distribution at the curved surface of an elastic finger," in *Proc. IEEE Int. Conf. Robot. Automat.*, Apr. 2000, pp. 3895–3900.
- [77] D. Yamada, T. Maeno, and Y. Yamada, "Artificial finger skin having ridges and distributed tactile sensors used for grasp force control," *J. Robot. Mechatronics*, vol. 14, no. 2, pp. 140–146, 2002.
- [78] Y. Yamada, H. Morita, and Y. Umetani, "Slip phase isolating: Impulsive signal generating vibrotactile sensor and its application to real-time object regrip control," *Robotica*, vol. 18, no. 1, pp. 43–49, 2000.
- [79] I. Fujimoto, Y. Yamada, T. Morizono, Y. Umetani, and T. Maeno, "Development of artificial finger skin to detect incipient slip for realization of static friction sensation," in *Proc. IEEE Int. Conf. Multisensor Fusion Integr. Intell. Syst.*, Aug. 2003, pp. 15–20.
- [80] G. Canepa, R. Petriglano, M. Campanella, and D. De Rossi, "Detection of incipient object slippage by skin-like sensing and neural network processing," *IEEE Trans. Syst. Man, Cybern. B, Cybern.*, vol. 28, no. 3, pp. 348–356, Jun. 1998.
- [81] A. Ikeda, Y. Kurita, J. Ueda, Y. Matsumoto, and T. Ogasawara, "Grip force control for an elastic finger using vision-based incipient slip feedback," in *Proc. IEEE/RSJ Int. Conf. Intell. Robots Syst.*, Sep./Oct. 2004, pp. 810–815.
- [82] J. Ueda, A. Ikeda, and T. Ogasawara, "Grip-force control of an elastic object by vision-based slip-margin feedback during the incipient slip," *IEEE Trans. Robot.*, vol. 21, no. 6, pp. 1139–1147, Dec. 2005.
- [83] N. Watanabe and G. Obinata, "Grip force control based on the degree of slippage using optical tactile sensor," in *Proc. Int. Symp. Micro-NanoMechatronics Hum. Sci.*, 2007, pp. 466–471.
- [84] Y. Ito, Y. Kim, and G. Obinata, "Robust slippage degree estimation based on reference update of vision-based tactile sensor," *IEEE Sensors J.*, vol. 11, no. 9, pp. 2037–2047, Sep. 2011.
- [85] H. William, Y. Ibrahim, and B. Richardson, "A tactile sensor for incipient slip detection," *Int. J. Optomechatronics*, vol. 1, no. 1, pp. 46–62, 2007.
- [86] Y. Tada and K. Hosoda, "Acquisition of multi-modal expression of slip through pick-up experiences," *Adv. Robot.*, vol. 21, nos. 5–6, pp. 601–617, 2007.
- [87] S. Shirafuji and K. Hosoda, "Detection and prevention of slip using sensors with different properties embedded in elastic artificial skin on the basis of previous experience," *Robot. Auton. Syst.*, vol. 62, no. 1, pp. 46–52, 2014.
- [88] A. Mamun and M. Y. Ibrahim, "New approach to detection of incipient slip using inductive sensory system," in *Proc. IEEE Int. Symp. Ind. Electron.*, Jul. 2010, pp. 1901–1906.
- [89] V. A. Ho and S. Hirai, "Modeling and analysis of a frictional sliding soft fingertip, and experimental validations," *Adv. Robot.*, vol. 25, nos. 3–4, pp. 291–311, 2011.
- [90] V. A. Ho, Z. Wang, and S. Hirai, "Beam bundle model of human-like fingertip for investigation of tactile mechanism," in *Proc. IEEE/RSJ Int. Conf. Intell. Robots Syst. (IROS)*, Nov. 2013, pp. 4491–4498.
- [91] W. Yuan, R. Li, M. A. Srinivasan, and E. H. Adelson, "Measurement of shear and slip with a GelSight tactile sensor," in *Proc. IEEE Int. Conf. Robot. Automat.*, May 2015, pp. 304–311.
- [92] S. Dong, W. Yuan, and E. H. Adelson. (Aug. 2017). "Improved GelSight tactile sensor for measuring geometry and slip." [Online]. Available: <https://arxiv.org/abs/1708.00922>
- [93] E. Donlon, S. Dong, M. Liu, J. Li, E. Adelson, and A. Rodriguez. (May 2018). "GelSlim: A high-resolution, compact, robust, and calibrated tactile-sensing finger." [Online]. Available: <https://arxiv.org/abs/1803.00628>
- [94] R. D. Howe and M. R. Cutkosky, "Sensing skin acceleration for slip and texture perception," in *Proc. IEEE Int. Conf. Robot. Automat.*, May 1989, pp. 145–150.
- [95] M. R. Tremblay and M. R. Cutkosky, "Estimating friction using incipient slip sensing during a manipulation task," in *Proc. IEEE Int. Conf. Robot. Automat.*, May 1993, pp. 429–434.
- [96] J. S. Son, E. A. Monteverde, and R. D. Howe, "A tactile sensor for localizing transient events in manipulation," in *Proc. IEEE Int. Conf. Robot. Automat.*, May 1994, pp. 471–476.
- [97] H. Khamis, R. I. Albero, M. Salerno, A. S. Idil, A. Loizou, and S. J. Redmond, "PapillArray: An incipient slip sensor for dexterous robotic or prosthetic manipulation—Design and prototype validation," *Sens. Actuators A, Phys.*, vol. 270, pp. 195–204, Feb. 2018.
- [98] K. Nakamura and H. Shinoda, "A tactile sensor instantaneously evaluating friction coefficients," in *Proc. 11th Int. Conf. Solid-State Sens. Actuators*, 2001, pp. 1430–1433.
- [99] K. Nakamura and H. Shinoda, "Tactile sensing device instantaneously evaluating friction coefficients," in *Tech. Dig. Sensor Symp.*, 2001, pp. 151–154.
- [100] H. Shinoda, S. Sasaki, and K. Nakamura, "Instantaneous evaluation of friction based on ARTC tactile sensor," in *Proc. IEEE Int. Conf. Robot. Automat.*, Apr. 2000, pp. 2173–2178.
- [101] T. Maeno, T. Kawamura, and S.-C. Cheng, "Friction estimation by pressing an elastic finger-shaped sensor against a surface," *IEEE Trans. Robot. Autom.*, vol. 20, no. 2, pp. 222–228, Apr. 2004.
- [102] T. Okatani, H. Takahashi, K. Noda, T. Takahata, K. Matsumoto, and I. Shimoyama, "A tactile sensor using piezoresistive beams for detection of the coefficient of static friction," *Sensors*, vol. 16, no. 5, p. 718, 2016.

- [103] W. Chen *et al.*, “An eight-legged tactile sensor to estimate coefficient of static friction,” in *Proc. 37th Annu. Int. Conf. IEEE Eng. Med. Biol. Soc. (EMBC)*, Aug. 2015, pp. 4407–4410.
- [104] W. Chen, H. Wen, H. Khamis, and S. J. Redmond, “An eight-legged tactile sensor to estimate coefficient of static friction: Improvements in design and evaluation,” in *Proc. Int. Conf. Hum. Haptic Sens. Touch Enabled Comput. Appl.*, 2016, pp. 493–502.
- [105] D. S. Chathuranga, Z. Wang, and S. Hirai, “Challenges in developing soft tactile sensors for robots that detect incipient slip,” in *Proc. 7th Int. Conf. Inf. Automat. Sustainability*, 2014, pp. 1–7.
- [106] L. Harmon, “Touch-sensing technology—A review,” *Soc. Manuf. Eng.*, Dearborn, MI, USA, Tech. Rep. MSR80-03, 1980.
- [107] J. Platkiewicz, H. Lipson, and V. Hayward, “Haptic edge detection through shear,” *Sci. Rep.*, vol. 6, Mar. 2016, Art. no. 23551.
- [108] M. R. Cutkosky, R. D. Howe, and W. R. Provancher, “Force and tactile sensing,” in *Springer Handbook of Robotics*, B. Siciliano and O. Khatib, Eds. Cham, Switzerland: Springer, 2016, pp. 717–736.
- [109] H. Khamis *et al.*, “Design principles for building a soft, compliant, high spatial resolution tactile sensor array,” in *Proc. 10th Int. Conf. Haptics, Perception, Devices, Control, Appl. (EuroHaptics)*. Cham, Switzerland: Springer, 2016, pp. 25–34.

Wei Chen received the bachelor’s degree in control science and engineering from Zhejiang University, China, in 2012, and the master’s degree by research in electrical and computer engineering from the University of Macau, China, in 2013. He is currently pursuing the Ph.D. degree with the Graduate School of Biomedical Engineering, University of New South Wales, Sydney, Australia. His primary research areas include biosignal processing and tactile sensing techniques, particularly tactile sensor design and fabrication. His current research project is focused on the design of friction sensors and their integration with real-time robotic manipulation systems.

Heba Khamis (M’15) received the bachelor’s of (software) engineering and bachelor’s of medical science degrees from the University of Sydney in 2007, and the Ph.D. degree in developing methods for epileptic seizure detection from EEG, School of Electrical and Information Engineering, University of Sydney, in 2011. She is currently a Lecturer with the Graduate School of Biomedical Engineering, University of New South Wales, Sydney, Australia. Her research interests include human tactile physiology, artificial tactile sensor design and robotic grip control, and photogrammetric anthropometry.



Ingvars Birznieks received the Ph.D. degree from Umeå University, Sweden, focusing on tactile sensory control of dexterous manipulation in humans. During his post-doctoral period, he moved to Australia, first to the University of Melbourne and then to the Neuroscience Research Australia, Sydney. After his post-doctoral studies, he established his own research laboratory and created an inter-disciplinary research network linking neuroscience, biomedical engineering, and clinical neurology. He is currently a Senior Lecturer with the School of Medical Sciences, University of New South Wales, Sydney, Australia, and a Senior Research Fellow with the Neuroscience Research Australia. He is also a Sensory Neurophysiologist interested in tactile sensory information encoding mechanisms.



Nathan F. Lepora received the B.A. degree in mathematics and the Ph.D. degree in theoretical physics from the University of Cambridge, U.K. He is currently a Reader (Associate Professor) with the Department of Engineering Mathematics, University of Bristol, U.K., where he leads the Bristol Robotics Laboratory, Tactile Robotics Group. His research interests span robotics and computational neuroscience, focusing on robot touch and animal perception, artificial and natural decision making, and biomimetics. He was the Program Chair of the International Conference of Living Machines in 2012, 2013, and 2016.



Stephen J. Redmond (M’07–SM’13) received the bachelor’s degree in electronic engineering and the Ph.D. degree in biosignal processing from the University College Dublin, Ireland, in 2002 and 2006, respectively. He is currently an Adjunct Associate Professor with the Graduate School of Biomedical Engineering, University of New South Wales, Sydney, Australia. He is interested in the application of signal processing and pattern recognition techniques to solve or better understand biomedical engineering problems. The principal application areas for these signal processing and pattern recognition techniques include telehealth, wearable technologies, and tactile sensing and physiology.